

# Dissecting the Role of the *IFIH1* Locus in Type 1 Diabetes using Genome Editing

## FINAL REPORT

Submitted at the

Austrian Marshall Plan Foundation



**Marshallplan-Jubiläumsstiftung**  
Austrian Marshall Plan Foundation

**Theresa BRANDSTETTER**

Bachelor program

*“Medical and Pharmaceutical Biotechnology”*

IMC Fachhochschule Krems

Supervised by: Dr. Torsten Meissner and Prof. Chad A. Cowan, PhD

Submitted on: 31.03.2017

## Acknowledgements

To begin with, I would like to express my deepest gratitude to Professor Chad A. Cowan, PhD at the Harvard Department of Stem Cell and Regenerative Biology, to give me the opportunity of doing my internship in his laboratory, and to gain my first scientific working experience.

Secondly, I am indebted to Dr. Torsten B. Meissner for being my mentor and adopting me in his research project. He taught me everything I needed to know and even more. His motivation and passion made me realize how much I actually like academic research; I soon developed my own passion for my small project, and felt honored when he asked for my help in his projects. He was always open for questions, no matter how stupid or complicated they were, and did not waste a single second to help me. Torsten was not only a mentor in lab, but also a friend during my whole internship, who encouraged, supported, but also criticized me whenever needed.

Thirdly, my deepest appreciation goes to Alana Allen, who has not only been a coworker in lab, but also the best friend I could imagine. She was very helpful from the first moment on, showed me “how to survive” in lab, and always answered my questions. She taught me that research does not always have to be serious, but can be a lot of fun. She definitely made my internship and stay in Cambridge unforgettable, especially when considering all those late-night gym moments, insider jokes, or crazy food cravings we shared.

Special thanks also to all the members of the Cowan and Strominger labs, who never hesitated to help if I had questions. I am glad that I had the opportunity to experience so many scientific relevant events, such as talks of various scientists doing research on the broadest variety of fields, lab meetings and journal clubs with them. Besides serious events, we also did a lot of enjoyable and fun things together, like the lab retreat in New Hampshire, or our skiing trip to Mount Washington. I would particularly like to thank Kiwi Florido, Max Friesen, Min Jin Lee, and Stanley Tam – the “Gang” – for welcoming me in their special group, all those endless nights

of Catan, Cards Against Humanity and Jenga, and all other wonderful activities we did together.

Furthermore, I am deeply grateful to the Harvard undergrads from the Cowan lab, Andrew Mazzanti, Kruti Vora, and Margaret Irwin for their mutual support concerning thesis writing and surviving the final year of college, and for giving me the opportunity to experience Black Friday Shopping and the life as a college student in the US.

I am also very thankful for the support I received from my home university, especially from my internal supervisor DI Bernhard Klausgraber, Dr. Barbara Entler for her excellent organizational work, and of course Dr. Harald Hundsberger, and the whole IMC team.

Moreover, I owe my deepest gratitude to my family and friends, who have always supported me, for being my safe haven.

Finally, I want to thank the Austrian Marshall Plan Foundation for their financial support, and by thereby making this great experience possible in the first place.

To summarize all this, I would like to end my acknowledgements part with a simple quotation:

“It is costly wisdom that is bought by experience.”

Roger Ascham

## Abstract

Type 1 Diabetes (T1D) is an autoimmune disease characterized by the selective immune-mediated destruction of the insulin producing beta cells in the pancreas. It accounts for 5% of all diabetes incidences, and in the United States alone, more than 1 million people suffer from the disease. A steady increase in T1D has been predicted, but so far, T1D can only be treated, but not cured. Moreover, despite decades of research, the cause of T1D is still unknown. It has been proposed that T1D is caused by both environmental and genetic risk factors. Environmental triggers include dietary habits, bacterial and most commonly viral infections. More than 50 T1D susceptibility loci have been identified in Genome Wide Association Studies (GWAS). One susceptibility gene in particular may represent a link between genetic T1D predisposition and environmental challenges: Interferon induced helicase 1 (*IFIH1*) encodes for the cytoplasmic viral sensor melanoma differentiation associate protein 5 (MDA5). Upon viral infection, MDA5 binds to double stranded RNA and induces a proinflammatory response by upregulating the expression of several interferons and interleukins. It has been proposed that the inflamed state of an infected pancreatic beta cell and the subsequent higher apoptotic rate may facilitate presentation of self-antigens to the immune system, thereby triggering the onset of T1D development. Several single nucleotide polymorphisms (SNPs) in the *IFIH1* locus have been identified. These rare *IFIH1* variants are protective against T1D and it seems plausible that the resulting truncated protein isoforms are less functional, and thereby result in a reduced immune response upon viral infection.

To test this hypothesis, we decided to generate a human T1D disease model by deleting the *IFIH1* gene in human embryonic stem (ES) cells and differentiating them into disease relevant cell types. We used the CRISPR-Cas9 genome editing system to specifically target the *IFIH1* gene and establish a disease model to better investigate the events that may trigger T1D onset. We decided on Endothelial Cells (ECs) and, obviously, pancreatic beta cells as being the most T1D related and relevant cell types for our disease model. Once our *IFIH1* knockout cell lines were generated, we differentiated them into ECs. We then mimicked viral infection by exposing ECs

to synthetic double stranded RNA (poly(I:C)). Subsequently, we tested the immune response of *IFIH1*-deficient ECs on either the mRNA or the protein level.

I was able to generate a homozygous ES cell line harboring a truncated MDA5 protein. Upon differentiation into EC, *IFIH1*-deficient cells showed an impaired anti-viral response as indicated by reduced induction of interferon beta, a target gene of the MDA5 signaling pathway. Furthermore, I generated a heterozygous *IFIH1* knockout cell line, which displayed a significant reduction in several target genes of the MDA5 pathway. Although, due to time constraints, I was not able to differentiate my cell lines into pancreatic beta cells, an activity ongoing in the Cowan lab, my results obtained in *IFIH1*-deficient ECs are very promising and suggest that they can be used for disease modelling and may contribute to a better understanding of the mechanisms of T1D onset.

# Table of Contents

Acknowledgements .....	II
Abstract.....	IV
Table of Contents.....	VI
List of Figures.....	VIII
List of Supplemental Figures.....	VIII
List of Supplemental Tables .....	VIII
List of Abbreviations.....	IX
1 Introduction .....	1
1.1 Statistical Hard Facts.....	1
1.2 Type 1 Diabetes .....	1
1.2.1 Pathogenesis .....	2
1.2.2 Causes.....	5
1.2.3 Genetics.....	8
1.2.4 Ways to Diagnose.....	12
1.2.5 Currently Available Treatment Options .....	13
1.3 Genome Editing using CRISPR/Cas9 .....	14
1.3.1 CRISPR-Cas9.....	15
1.4 Hypothesis.....	15
2 Materials and Methods.....	17
2.1 Designing CRISPR guide RNA plasmids.....	17
2.2 Cloning of CRISPR gRNAs .....	17
2.3 Transformation into Escherichia coli Competent Cells .....	17
2.4 Small Scale DNA Isolation (Mini Prep) .....	18
2.5 Large Scale DNA Isolation (Maxi Prep).....	18
2.6 Maintenance/Propagation of HEK 293T Cells .....	18
2.7 Transfection of HEK 293T Cells .....	19
2.8 Polymerase Chain Reaction (PCR) Amplification.....	19
2.9 Gel Electrophoresis .....	19
2.10 Gel Elution and Sequencing.....	20
2.11 Maintenance/Propagation of HuES8 Cells .....	20
2.12 Electroporation of HuES8 Cells .....	20
2.13 Determination of Genome Edited Cells .....	20

2.14	Large Scale Screening for Knockout Clones .....	21
2.15	Differentiation of HuES8 into Endothelial Cells.....	21
2.15.1	Protocol 1 .....	22
2.15.2	Protocol 2.....	23
2.16	Flow Cytometry Staining and Analysis .....	24
2.17	Poly(I:C) Treatment of Endothelial Cells.....	24
2.18	RNA Isolation .....	25
2.19	cDNA Synthesis .....	25
2.20	Quantitative Real Time PCR .....	25
2.21	Western Blot.....	25
2.22	Statistical Analysis.....	26
3	Results .....	27
3.1	Specific Deletion of IFIH1 Start Codon.....	27
3.2	Successful Differentiation and Enrichment of HuES8 Derived Endothelial Cells .....	31
3.3	qPCR and Western Blot Reveal Residual IFIH1 mRNA and MDA5 Protein Expression.....	33
3.4	Revised IFIH1 Targeting Approach .....	34
4	Discussion.....	40
	List of References .....	44
	Annex.....	47

## List of Figures

Figure 1: Possible pathogenesis of T1D. ....	3
Figure 2: T1D and the immune system. ....	5
Figure 3: T1D susceptibility genes. ....	10
Figure 4: MDA5 signaling pathway.....	11
Figure 5: Flow chart EC differentiation Protocol 1..	22
Figure 6: Flow chart of EC differentiation Protocol 2. ....	23
Figure 7: <i>IFIH1</i> targeting strategy.....	28
Figure 8: Deletion of <i>IFIH1</i> start codon in HuES8. ....	30
Figure 9: Flow Cytometry analysis of MACS enriched ECs (protocol 1). ....	32
Figure 10: Determination of <i>IFIH1</i> and MDA5 expression in WT and KO ECs.....	34
Figure 11: Deletion of entire <i>IFIH1</i> gene by revised targeting approach. ....	36
Figure 12: Flow Cytometry analysis of MACS enriched ECs (protocol 2). ....	38
Figure 13: qPCR to determine mRNA levels after mimicking viral infection; .....	39
Figure 14: Structural considerations of MDA5.....	42

## List of Supplemental Figures

Supplemental Figure 1: Plasmids used in this study. ....	47
--	----

## List of Supplemental Tables

Supplemental Table 1: List of gRNAs used. ....	47
Supplemental Table 2: List of primers.....	48
Supplemental Table 3: List of antibodies used for Flow Cytometry.....	49
Supplemental Table 4: List of antibodies used for Western Blot. ....	49

## List of Abbreviations

T1D	Type 1 Diabetes
T2D	Type 2 Diabetes
Treg	Regulatory T cell
APC	Antigen presenting cell
MHC	Major histocompatibility complex
IFN	Interferon
DC	Dendritic cells
IL	Interleukin
NK	Natural killer
IPEX	Immune dysfunction, polyendocrinopathy, enteropathy, X-linked inheritance
EV	Enterovirus
CVB	Coxsackievirus B
CAR	Coxsackievirus and adenovirus receptor
DAF	Decay-accelerating factor
GAD	Glutamic acid decarboxylase
ds	Double-stranded
TLR3	Toll like receptor 3
MDA5	Melanoma differentiation associated protein 5
NOD	Non-obese diabetic
GWAS	Genome Wide Association Study
HLA	Human Leukocyte Antigen
INS	Insulin gene
VNTR	Variable number of tandem repeat
poly(I:C)	Synthetic double-stranded RNA
IL2RA	Interleukin-2 receptor $\alpha$

CTLA-4	cytotoxic T lymphocyte-associated protein 4
<i>IFIH1</i>	Interferon induced helicase C domain 1
SNP	Single nucleotide polymorphism
A1C	Glycated hemoglobin
CRISPR	Clustered regularly interspaced short palindromic repeats
Cas	CRISPR-associated
RGEN	RNA-guided engineered nuclease
ZFN	Zinc-finger nuclease
TALEN	Transcription activator-like effector nuclease
PAM	protospacer adjacent motif
crRNA	CRISPR RNA
tracrRNA	trans-activating crRNA
DSB	Double strand break
SpCas9	<i>Streptococcus pyogenes</i> Cas9
sgRNA	Single guide RNA
gRNA	Guide RNA
PCR	Polymerase Chain Reaction
HuES8	Human Embryonic Stem cell line 8
EC	Endothelial Cell
WT	Wildtype
KO	Knockout
MFI	Mean fluorescence intensity
CTD	Carboxy-terminal domain
Hel	Helicase

# 1 Introduction

## 1.1 Statistical Hard Facts

415 million people around the world suffer from diabetes, and approximately 5% of them are Type 1 Diabetes (T1D) patients<sup>1</sup>. Although both T1D and Type 2 Diabetes (T2D) lead to the same symptoms and further complications, due to cells losing the ability to take up glucose, the causes are different: in T2D the body develops insulin resistance due to permanently high blood glucose levels<sup>2</sup>, whereas in T1D autoimmunity results in the destruction of insulin-producing pancreatic beta cells<sup>3</sup>.

1.25 million Americans are diagnosed with T1D, among them approximately 200,000, who are less than 20 years of age. Each year, 40,000 new T1D cases are reported, and by 2050, it is estimated that 5 million Americans will suffer from the disease. A steady increase of T1D incidences has been reported, and in the United States only, T1D accounts for 14 Billion Dollars annual health costs, considering that, until now, T1D can only be treated, but not cured. Without treatment, T1D will inevitably lead to dangerous health complications and death<sup>4</sup>.

## 1.2 Type 1 Diabetes

T1D, a form of diabetes mellitus, is a multifactorial disease caused by the selective immune-mediated destruction of insulin-producing pancreatic beta cells. The subsequent lack of insulin prohibits glucose uptake by the body's tissue<sup>5</sup>. A typical symptom of T1D is elevated blood sugar (hyperglycemia), which is also the main symptom of T2D<sup>3</sup>. T1D was regarded as lethal until the exact role and importance of insulin concerning the regulation of the blood glucose level was discovered. Subsequently, exogenous insulin therapy was developed<sup>6</sup>. Unlike in T2D, in which insulin resistance is caused by obesity and other factors<sup>2</sup>, T1D is an autoimmune disease, with both the humoral and cellular immune system involved<sup>7</sup>. It is usually diagnosed in people younger than 20-30 years of age, and thus it is also referred to as juvenile-onset diabetes. The incidence rates rise from birth, show a peak at the

age of about 14, decrease after adolescence, and finally stabilize in adults<sup>8</sup>. The three most common symptoms are polydipsia (enhanced thirst), subsequent polyuria (recurrent urination) and polyphagia (hunger)<sup>9</sup>. Untreated T1D can lead to fatal health complications such as heart disease, stroke, kidney failure, ketoacidosis and retinopathy<sup>7,8</sup>.

So far many registered studies on T1D have been conducted, including the World Health Organization Multinational Project for Childhood Diabetes (DIAMOND Project), SEARCH for Diabetes in Youth, The Environmental Determinants of Diabetes in the Youth (TEDDY), BABYDIAB, the Finnish type 1 Diabetes Prediction and Prevention (DIPP), and the American Diabetes Autoimmunity Study in the Young (DAISY), just to name a few<sup>7,8</sup>.

### **1.2.1 Pathogenesis**

Many models have been put forward to explain the interplay between genetic and environmental triggers of the T1D. The most common, and most referenced model is that of Eisenbarth in 1986, which proposes a linear decay of beta cells in genetically susceptible individuals after being confronted with a certain environmental trigger. This then results in islet autoimmunity, development of autoantibodies, and hyperglycemia. Some authors object T1D progression being a linear progress, but it differs in every individual patient. Van Belle et al. introduced a more detailed version of non-linear T1D pathogenesis (Figure 1), proposing that a disequilibrium between autoreactive effector T cells and regulatory T cells (Tregs) could develop over time. This shift in equilibrium might then eventually lead to a decrease in beta cell mass<sup>3</sup>.

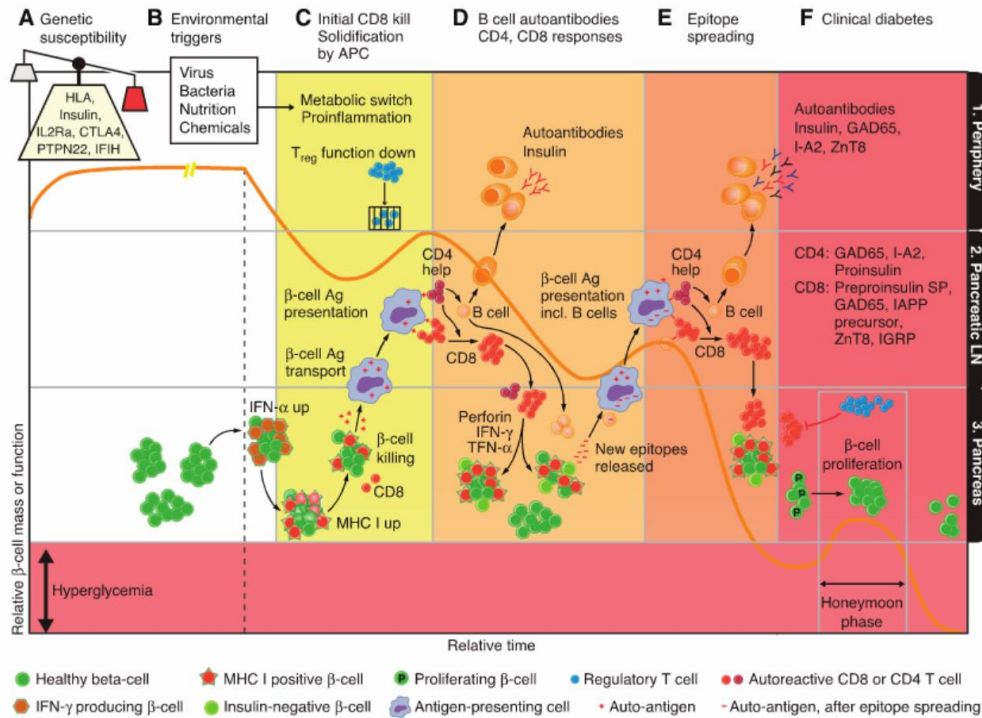


**Figure 1: Possible pathogenesis of T1D.**

This figure illustrates the possible pathogenesis of T1D, on a cellular level, as proposed by Van Belle et al. <sup>3</sup>

Clinical diabetes is not present until 80-90% of the total beta cell mass has been lost, but as T1D is an ill-defined autoimmune disease it is not completely known how the development occurs. However, new studies show that in some individuals 40-50% of the beta cells are still viable at the onset of hyperglycemia<sup>9</sup>.

The development of T1D is a complex set of events including activation of antigen-presenting cells (APCs) that present beta cell antigens, islet destruction and subsequent insulin deficiency. It is believed that infection, either direct infection of the beta cells (insulinitis) with subsequent destruction, or through creating a “fertile field” for immune responses might be the causative events leading to T1D<sup>6</sup>. The fertile field (time window following viral infection) is thought to allow autoreactive T cells to increase in number by various mechanisms, such as molecular mimicry, and lead to full autoimmunity and T1D<sup>3</sup>. Infection would subsequently lead to upregulation of major histocompatibility complex (MHC) class I and proinflammatory cytokines, for example interferon (IFN)- $\alpha$ . These proinflammatory cytokines affect the beta cells

and lead to upregulation of chemokine expression. Dendritic cells (DCs), which are present in the islets at any given time, can take up released beta cell antigen. The latter are also activated and promoted to present beta cell antigens to T cells by type I IFNs<sup>6</sup>. Presentation of beta cell antigens might additionally be caused by any type of beta cell insult including endoplasmic reticulum stress, apoptosis, necrosis, or autophagy<sup>10</sup>. DCs further activate CD4<sup>+</sup> T cells which can further activate islet antigen-specific B cells, which subsequently turn into antibody-producing plasma cells. The auto-antibodies will then bind to the beta cells and induce complement-mediated killing. Moreover, activated B cells function as antigen-presenting cells, which will lead to further enhancement of the anti-beta-cell immune response. The DCs, after interaction with beta cell antigen-specific CD4<sup>+</sup> T cells and the presence of proinflammatory cytokines, are induced to cross-present antigen to beta cell antigen-specific CD8<sup>+</sup> T cells, which will subsequently upregulate their cytotoxic properties and destroy beta cells<sup>6</sup>. All these events underlie the fact that T1D patients have several defects in their regulatory mechanisms that would keep autoreactive cells escaping negative selection in the thymus in healthy patients<sup>9</sup>.

Tregs and interleukin (IL)-4 producing natural killer (NK) cells are thought to alleviate the previously mentioned immune mechanisms. Tregs are characterized by expression of the forkhead box transcription factor Foxp3, and in humans loss-of-function mutations lead to immune dysfunction, polyendocrinopathy, enteropathy, X-linked inheritance (IPEX), a severe multiorgan autoimmune and inflammatory disorder. Treg produce immunosuppressive cytokines, such as IL-10 and TGF- $\beta$  (important for achieving immunological tolerance), and are able to kill APCs by releasing cytotoxic granules<sup>6</sup>. A schematic representation of the immunological events during T1D development can be seen in Figure 2 below.

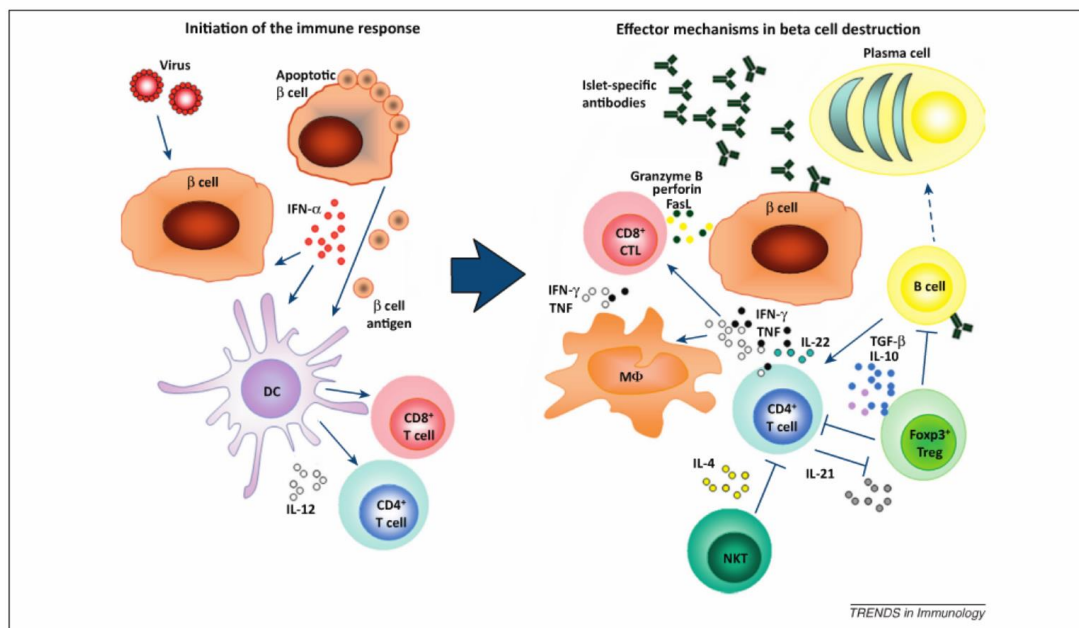


**Figure 2: T1D and the immune system.**

Schematic depiction of several immune mechanisms involved in beta cell destruction in T1D<sup>6</sup>.

## 1.2.2 Causes

Unlike other autoimmune diseases, including autoimmune polyendocrinopathy syndrome type I, Autoimmune Lymphoproliferative Syndrome, and the previously mentioned IPEX<sup>6</sup>, T1D is a very complex and multifactorial disease, triggered by both environmental and genetic risk factors. The most probable scenario is that environmental triggers induce T1D in individuals with genetic susceptibilities<sup>3,9</sup>.

### 1.2.2.1 Environment

Many hypotheses explaining the role of the environment in T1D and its pathogenesis have been proposed:

- The “accelerator” and “overload” hypotheses imply that certain environmental stresses (e.g. childhood obesity) might increase insulin demand and subsequently overload the beta cells accompanied with accelerated beta cell damage.

- The “hygiene hypothesis” proposes that a cleaner and more hygienical lifestyle suppresses the immune system, which would make individuals more prone to autoimmune diseases.
- According to the “fertile field” hypothesis microbial infection causes a momentary state during which other antigens can more easily prompt an immune response<sup>8,9</sup>.

#### 1.2.2.2 Bacteria

It is not clear to what extent gut bacteria contribute to T1D development, but it is believed that T1D is influenced by antibiotics and probiotics by changing the balance of gut microbiota<sup>3</sup>.

#### 1.2.2.3 Dietary Products

The most predominant dietary product considering T1D development is cow’s milk. Its high albumin content was found to cause cross-reactivity between serum antibodies to albumin and a certain beta cell surface protein. Other studies propose that early introduction of cow’s milk, as opposed to prolonged duration of breastfeeding might be a reason for autoimmunity, since there is evidence that breast-fed babies are better protected against enterovirus infections<sup>3</sup>.

Furthermore, although to a smaller extent than cow’s milk, wheat gluten is thought to play a role in T1D susceptibility, since a study has shown increased islet auto-antibody risk in children with T1D parents, after consuming gluten before the age of 3 months.

Finally, sun exposure and or Vitamin D intake – or rather the lack thereof – may contribute to T1D development. Vitamin D is thought to be protective against T1D by having immunosuppressive properties. Moreover, countries with higher levels of sunlight and therefore increased Vitamin D synthesis have a lower incidence for the autoimmune disease. Recent studies also show that polymorphisms in Vitamin D metabolism genes might interfere with T1D development<sup>3,8,9</sup>.

#### 1.2.2.4 Viruses

Viruses are probably the most investigated environmental factor in T1D progression. Several viruses comprising cytomegalovirus, Epstein-Barr virus, mumps virus, rotavirus, and rubella virus are considered environmental factors that trigger development of T1D. Moreover, there is clear evidence that Enteroviruses (EVs) and especially Coxsackievirus B (CVB) are linked to the disease<sup>11</sup>.

The viral genus of Enterovirus is part of the Picornaviridae family and has a total of more than 100 serotypes, including poliovirus, and Coxsackievirus. EVs are positive-sense, single-stranded, non-enveloped RNA viruses and their infections are very common in humans, with billions of cases every year. Among mild respiratory and gastrointestinal symptoms, also more severe acute inflammatory diseases, comprising myocarditis, meningitis, poliomyelitis and pancreatitis can occur following EV infection. Transmission mainly occurs via the fecal-oral route, and the major site of replication is the gut, but also secondary target organ sites, like the pancreas, are possible<sup>11,12</sup>.

It is believed that EV infections may play a role at either initiation of autoimmunity, or progression from islet autoimmunity to clinical onset of T1D, or even both; albeit it remains an open question if this is the case in every patient<sup>13</sup>. Several hypotheses of the exact role of EV or CVB in the pathogenesis of T1D have been established. CVBs are thought to enter the host cells by primarily using the Coxsackievirus and adenovirus receptor (CAR), as well as the decay-accelerating factor (DAF), with CAR being a tight-junctional component expressed in beta cells. Furthermore, antibodies against CAR can prevent enteroviral infection *in vitro*. Conversely DAF's physiological role is less clear, and interestingly, it is not expressed in islet cells. To explore the role of viral infection in development of autoimmunity and beta cell destruction a plausible mechanism by which these processes are linked must be provided. One possible mechanism is molecular mimicry, implying short sequence similarities between viral and islet proteins. For example, there are resemblances between a conserved sequence of the P2-C protein of CVB4 and one of the principal T1D autoantigens, glutamic acid decarboxylase (GAD)<sup>11,12</sup>.

After the EV escapes its initial site of infection (intestine) and infects the beta cells, it would lead to production of type I IFN, and proinflammatory cytokines, favoring both apoptosis and overexpression of MHC class I antigens, with the latter being a hallmark in T1D patients<sup>13</sup>. Usually EV infection and replication in host cells results in large scale cell lysis, but certain serotypes can replicate without destroying the cell. Moreover, it is reported that some CBV strains can persist in human beta cells, due to 5' terminal deletions of their genome, resulting in slower viral replication and further loss of cytopathic effect. The subsequent generation of double-stranded (ds) RNA during the viral replication process triggers an innate immune response by activating certain dsRNA sensors including Toll like receptor 3 (TLR3), retinoic-acid-inducible gene I, protein kinase R and melanoma differentiation associated protein 5 (MDA5). By stimulation of these viral sensors, pro-inflammatory cytokine production (including IL-1 $\alpha$  and  $\beta$ , IL-6, IL-8, TNF- $\alpha$ , type I IFNs) is induced, leading to inflammation. Because of increased IFN secretion MHC class I is hyperactivated in islet cells. It has been shown that MHC class I is upregulated in recent-onset T1D patients, and moreover the same was observed in the islets of non-obese diabetic (NOD) mice. The latter favors the presentation of viral antigens at the cell surface of the infected beta cells to professional APCs. The overexpression of MHC class I could also increase the recognition of islet cell autoantigens, due to the damage of the viral infection by autoreactive CD8<sup>+</sup> T cells<sup>11,12</sup>.

There are many other hypotheses about the exact role of EVs or CVB in the development of T1D, for example the possibility of the virus infecting thymic cells and thereby impairing proper T cell maturation and differentiation<sup>11</sup>. Nevertheless the previously described hypothesis is by far the most widely accepted, despite several arguments against it, such as the fact that not every person being infected by EVs also develops T1D<sup>12</sup>. One reason for this is that T1D is not only caused by environmental triggers, but it results from a complex interplay between those triggers, the immune system itself, and genetic susceptibility<sup>13</sup>, which will be further discussed.

### **1.2.3 Genetics**

Around 50 genetic loci which influence T1D development, were identified by Genome Wide Association Studies (GWAS), yet most of the mechanisms of how they

contribute to disease onset and development remain unknown. 40% of the T1D susceptibility loci are expressed in human islets or beta cells, where they are thought to influence the beta-cell response to the immune system. Also, 80% of the heritability of T1D is explained by these loci (<https://t1dbase.org/>). Moreover, it is proposed that gene expression may be regulated by genetic variations or epigenetics changes. Additionally, non-coding RNAs have recently been implicated in T1D development<sup>5</sup>.

#### 1.2.3.1 Genes Expressed in Immune Cells and Pancreatic Beta Cells

The most critical susceptibility locus is the Human Leukocyte Antigen (HLA) region located on chromosome 6, providing the greatest contribution of over 60% to the total genetic susceptibility. HLA class II genes code for molecules actively participating in antigen presentation and hence are strongly associated with T1D development. It is thought that different presentation of beta-cell antigens may promote anti-self-reactivity. These hypotheses are supported by the fact that about 40-50% of T1D patients harbor the disease associated HLA class II DR and DQ alleles. There are several genes that provide higher development risk, but only 1% of patients have alleles conferring protection against T1D. On the other hand, albeit to a lesser extent, class I alleles have been associated with T1D development, with HLA-B and HLA-A genes being the most prominent ones<sup>3,8,9</sup>.

Secondly, the insulin gene (INS) is not only a major autoantigen in T1D, but also a susceptibility gene, mapping to a variable number of tandem repeat (VNTR) polymorphism region on chromosome 11. VNTR class I alleles are proposed to predispose to, whereas class II alleles are said to protect from the onset of T1D<sup>5</sup>.

Further susceptibility genes are PTPN22, encoding for the lymphoid protein tyrosine phosphatase, which is also associated with other autoimmune diseases. It is upregulated by cytokines and synthetic dsRNA (polyinosinic: polycytidylic acid, poly(I:C)), and a gain-of function mutation, which suppresses T-cell receptor signaling is believed to allow autoreactive T cells to escape negative selection during thymic development. Also, the interleukin-2 receptor  $\alpha$  (IL2RA) was identified in several GWAS. Being expressed on T cells and Tregs depending on IL-2 for growing and

surviving, polymorphisms in *IL2RA* explain functional defects in Treg. Another gene identified in the GWAS and being confirmed as a risk allele encodes for the cytotoxic T lymphocyte-associated protein 4 (CTLA-4), which is a molecule ensuring proper negative regulation of immune responses<sup>3,5</sup>.

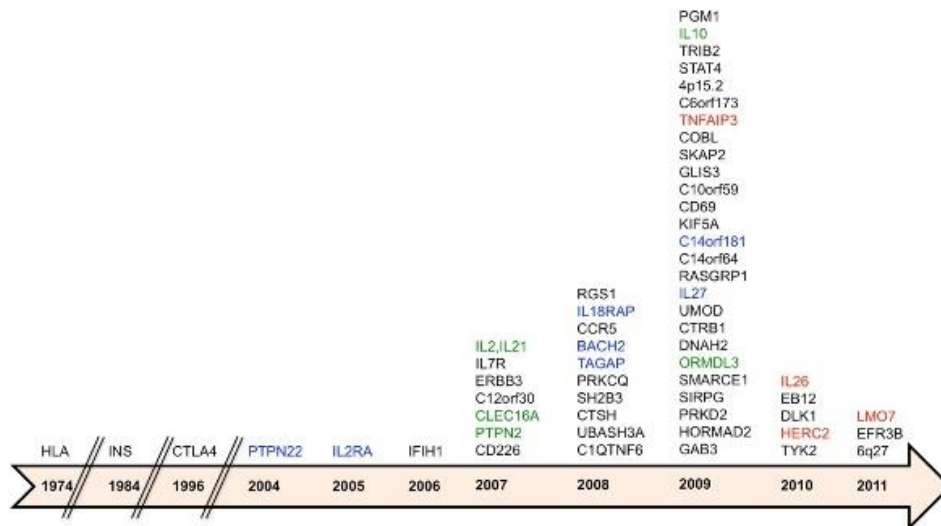


**Figure 3: T1D susceptibility genes.**

This figure shows a time line of all identified T1D susceptibility genes from 1974 until 2011<sup>14</sup>.

Many other susceptibility genes have been identified (see **Figure 3**) over the years of T1D research, and there are probably still many other genes involved, which have not been associated with the disease so far. But the gene that has attracted the most attention in T1D research is probably *IFIH1*, discussed in more detail below.

### 1.2.3.2 *IFIH1* – Linking Environmental and Genetic Risk Factors

Interferon induced helicase C domain 1 (*IFIH1*) codes for the intracellular viral RNA sensor MDA5, and has also been identified to be a major T1D susceptibility gene. Since MDA5 plays a crucial role in sensing viral dsRNA during viral infection *IFIH1*, it may build the bridge between environmental triggers and genetic predisposition to T1D<sup>15</sup>. The MDA5 protein has a dsRNA binding pocket and forms helical filaments along dsRNA<sup>16</sup>.

After sensing viral dsRNA, MDA5 recruits the mitochondria-bound protein MAVS, which activates several transcription factors, including IRF7, IRF3, IRF1 and NFκB, thereby initiating transcription of several pro-inflammatory cytokines, and INF-α/β/λ. Binding of INF-α or β activates a positive feedback loop by again initiating transcription of *IFIH1* and consequently the production of MDA5. Pro-inflammatory cytokines activate T and NK cells' cytolytic function, and recruit lymphocytes, monocytes and dendritic cells, which contribute to an inflammatory state leading to beta cell disruption by cytotoxic T and NK cells<sup>16,17</sup>, as seen in Figure 4.

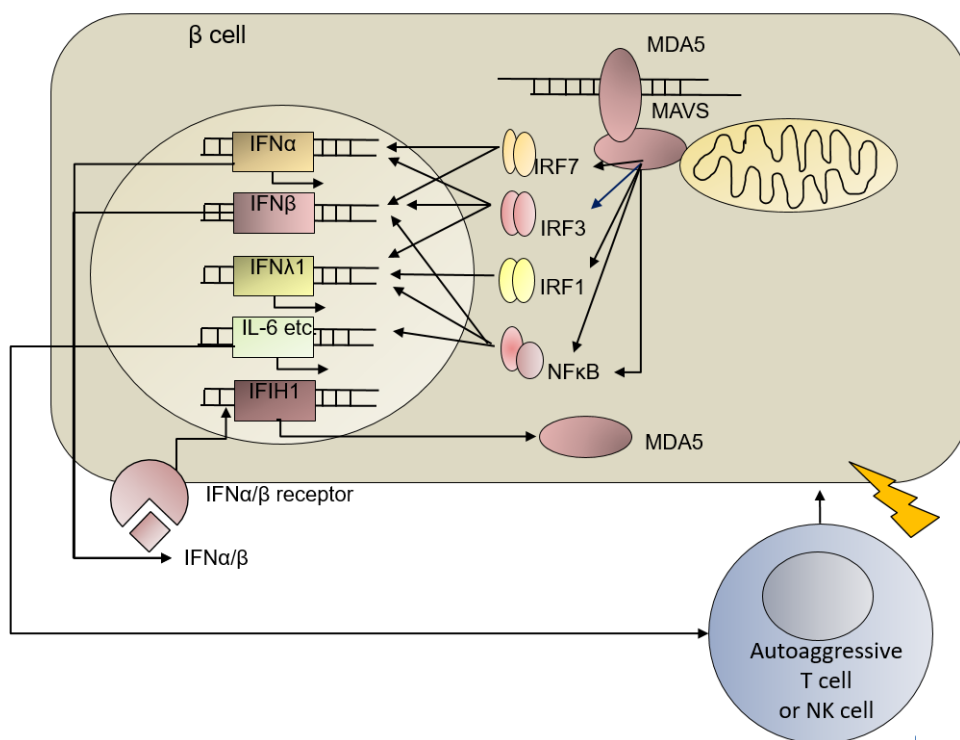


**Figure 4: MDA5 signaling pathway**

*MDA5 binds dsRNA and associates with the mitochondrial membrane bound protein MAVS, which further initiates expression of several proteins including interferons, and interleukins. Additionally it enhances the upregulation of IFIH1 by a positive feedback loop; modified from<sup>16,17</sup>.*

It was shown that there is a correlation between *IFIH1* single nucleotide polymorphisms (SNPs) and T1D, and gene expression is higher in individuals harboring these mutations. Hence the hypothesis arises that viral infections in patients with

elevated MDA5 levels are primarily perceived by the MDA5 pathway, thereby leading to an intensified antiviral response and secretion of interferons and interleukins. Moreover, rare protective variants have been identified. The latter lead to a truncated protein, which subsequently shows reduced function<sup>3,15</sup>. Noteworthy, *IFIH1* knockout NOD mice were protected from the development of T1D, and MDA5<sup>+/-</sup> heterozygous mice showed a reduced incidence rate, compared to wild type mice after viral infection<sup>15</sup>.

#### **1.2.4 Ways to Diagnose**

As already mentioned, clinical T1D onset occurs only after the vast-majority of beta cells have been destroyed, and pre-diabetes is symptom-free. The most common symptom of T1D is hyperglycemia, which is the result of the lack of insulin<sup>18</sup>. Common tests to determine the blood sugar level are the glycosylated hemoglobin (A1C), the random blood sugar, and the fasting blood sugar test. In the A1C test the average blood sugar of the last months is determined, where elevated levels are a clear indication of T1D. If the blood sugar level is above 200mg/dl (random blood sugar test), and 100-125mg/dl (fasting blood sugar test) clinical T1D can be assumed<sup>19</sup>.

Since it is desired to silence the attack of the beta cells at very early stages of T1D to achieve actual treatment, and T1D cannot be diagnosed before clinical onset, it is crucial to predict the disease. Firstly, genetic screening for the aforementioned SNPs in the susceptibility genes would be one possibility to do so. Secondly, autoantibodies, more explicitly, several, are considered the most predictive and reliable way. There are many T1D associated autoantibodies, with many of them being islet cell autoantibodies. The most prominent of the latter are autoantibodies against GAD, insulin, transmembrane tyrosine phosphatase and the zinc transporter 8. Typically, T1D associated autoantibodies are found in 70-80% of newly diagnosed patients, whereas only in 0.5% of the general population, and 3-4% of their relatives' serum show them. Additionally, the presence of two or more autoantibodies increases the risk for T1D<sup>3,9</sup>. Finally, T cell assays, which can distinguish between responses of T1D patients and healthy controls, and are performed on peripheral blood were reported to have high accuracy<sup>3</sup>.

### 1.2.5 Currently Available Treatment Options

Today it is only possible to treat, but not to cure T1D. The most common treatment option is exogenous insulin therapy by either syringes or an insulin pump. Since the insulin-producing beta cells are destroyed and cannot produce their own insulin anymore, the patients have to inject it. There are several types of insulin available, for example rapid-acting insulin, regular, or short-acting insulin, intermediate-acting insulin and long-acting insulin. To determine the right amount and strength of exogenous insulin it is of major importance to always monitor the blood glucose level. As an alternative for insulin injections, insulin pumps can be used. They are small computerized devices that can deliver insulin either in a steady dose, or as a so-called surge dose after meals. These doses are delivered through a plastic tube (catheter), which is permanently inserted through the skin into the fat tissue of the abdomen. Despite the insulin pump seeming to be very convenient, the risk of a sudden hypoglycemia (too low blood sugar) remains. Hypoglycemia is often referred to as an insulin shock, and in severe cases might even lead to coma or death<sup>18</sup>.

A very new method of glucose-sensing is the Glucose-Sensing Contact Lens, for which Google recently received a patent. The system will most likely consist of two or three parts, with part one being the contact lens itself, part two being a reading device, and part three being a display for the data to be shown and reviewed<sup>20</sup>.

More “old fashioned”, but rather invasive methods for treating T1D are transplantations, including both pancreas as well as islet transplantations. Pancreas transplantation was first performed 50 years ago, and accordingly the rates of graft acceptance and patient survival were rather low. But since surgical methods were improved significantly in recent years it is now a very common procedure with more than 10,000 transplanted pancreases until 1997. There are several different options for pancreatic transplantation, including the simultaneous transplantation with a kidney, pancreas transplantation after kidney transplantation, and pancreas-only transplantations, the least common procedure. Although a transplantation would eliminate the need of exogenous insulin injections, as well as the constant glucose monitoring it would also require lifelong immunosuppression to prevent organ rejection. These immunosuppressive drugs mostly come with severe side effects, hence a

transplantation is only recommended for patients after 20 years of established T1D, and if they show a history of frequent and acute metabolic complications and problems with exogenous insulin. Islet transplantation is far less invasive, but nonetheless also requires immunosuppression for lifetime. Furthermore, allograft transplantation frequently fails, probably because of impaired initial engraftment, or inflammatory response. Additionally, the immunosuppressive drugs may induce beta cell toxicity<sup>21,22</sup>.

### **1.3 Genome Editing using CRISPR/Cas9**

Clustered regularly interspaced short palindromic repeats (CRISPR)-CRISPR associated (Cas) system is a RNA-guided engineered nuclease (RGEN), and unlike Zinc-finger nucleases (ZFNs) and Transcription activator-like effector nuclease (TALENs) it has a natural origin. It was discovered to be the bacterial equivalent to an adaptive immune system, being used by 50% of bacteria and 90% of archaea. Microbes are able to acquire genetic records of invaders, such as bacteriophages, to ensure a quick “immune response” upon reinfection. CRISPR loci typically comprise a clustered set of CRISPR-associated genes and the signature CRISPR array. The latter is a series of direct repeats separated by variable sequences, the so-called spacers. It was discovered that the spacers are derived from viral genomes, and are thereby corresponding to sequences within foreign genetic elements (protospacers). It was demonstrated that a spacer, which matches the protospacer of a phage genome gives immunity to the host bacteria against the corresponding phage and infection also leads to the subsequent expansion of the CRISPR-array by inserting new spacers into the bacterial genome. Nonetheless the selection of new protospacer sequences of the foreign invading genome is not random, but the sequence requires the presence of a 2-5 nucleotide protospacer adjacent motif (PAM), which is located right next to the protospacer sequence. The CRISPR arrays are transcribed as a single RNA and further processed into shorter CRISPR RNAs (crRNAs), which, together with an invariable target-independent trans-activating crRNA (tracrRNA), direct the activity of the Cas enzymes, to degrade the target DNA. The Cas genes are translated, as already mentioned, into proteins, and they are the active part of the CRISPR-Cas system by harboring endonucleolytic functions<sup>23</sup>. For

CRISPR-Cas systems Types I, III, and IV, their signature Cas proteins are multi-subunit effector complexes, whereas those of Types II, V, and VI are single-subunit effectors<sup>23-25</sup>. The CRISPR-Cas9 system is one of the best studied, and widely used CRISPR-Cas systems, hence the further emphasis will be put on the latter.

### 1.3.1 CRISPR-Cas9

Cas9 functions as a single protein, together with the crRNA and tracrRNA, and cleaves DNA at the target site, leading to a double strand break (DSB). It consists of two distinct lobes, with the nuclease lobe having the function to cleave the target, and non-target strand, and the  $\alpha$ -helical lobe, whose function is the interaction with the guide RNA. Cas9 continuously scans the genome for an appropriate PAM, and initiates unwinding of the target DNA, where a perfect, or near-perfect concordance with the guide RNA leads to DSBs<sup>24</sup>.

In 2012, it was shown that the CRISPR-Cas9 system, due to its ability to cleave target DNA, can also be used for genetic engineering, by just changing the guide RNA sequences. The most used Cas protein is the *Streptococcus pyrogenes* Cas9 (SpCas9), which has proven efficiency in a variety of species and cell types, including human cell lines, primary cells, bacteria, zebrafish, yeast, and mouse, just to name a few. SpCas9 can be fused with either a pair of crRNA and tracrRNA, or with a single guide RNA (sgRNA), requiring to contain a 20bp nucleotide sequence corresponding to the target site. As already mentioned, Cas9 requires the presence of a PAM immediately downstream of the target site to actually cleave the DNA<sup>23,24,26</sup>. The PAM of SpCas9 is 5'-NGG-3'<sup>27</sup>.

## 1.4 Hypothesis

Despite decades of research, the exact mechanism of T1D onset remains unknown. Although not proven, it is very likely that T1D is caused by an interplay of environmental and genetic risk factors. After compiling many facts about T1D and its onset, *IFIH1* attracted more and more of our attention: It encodes for a cytoplasmic viral sensor, MDA5, which triggers an intense immune response upon viral infection. It

has been reported that viral infections, especially those of EV are linked to the disease. Moreover, several SNPs in the *IFIH1* locus have been identified. Four of those SNPs were shown to be protective against T1D, since they result in a truncated, and less functional protein. Considering all those facts, we hypothesize that *IFIH1* might be a major player in disease development, by linking genetic and environmental triggers. Furthermore, we predict, *IFIH1* knockout will prevent stem cell-derived human T1D disease relevant cells from an overshooting stress response after viral challenge, which may protect them from T1D disease onset.

## 2 Materials and Methods

### 2.1 Designing CRISPR guide RNA plasmids

The CRISPR guide RNAs (gRNAs) were designed using the MIT CRISPR design (<http://crispr.mit.edu/>) online tool that uses a special algorithm to select CRISPR gRNAs considering possible off-targets.

### 2.2 Cloning of CRISPR gRNAs

Oligonucleotides encoding the respective gRNAs were annealed using a master mix containing 6.5µl H<sub>2</sub>O, 1µl 10x T4 Ligation Buffer (NEB), 1µl gRNA oligonucleotide (10µM), 1µl reverse complement gRNA oligonucleotide (10µM), 0.5µl T4 PNK (NEB). The following conditions were used:

#### Annealing

37	30min
95	05min
↓	5°C/5min
25	hold

The annealed gRNAs oligonucleotides were diluted 1:200 and ligated using a master mix containing 6.5µl H<sub>2</sub>O, 1µl 10x T4 Ligation Buffer (NEB), 1µl lentiGuide-Puro vector (Plasmid #52963, Addgene), 1µl gRNA oligonucleotide and 0.5µl T4 DNA Ligase (NEB). Ligation was completed after 1 hour at room temperature.

### 2.3 Transformation into *Escherichia coli* Competent Cells

30µl of *Escherichia (E.) coli* competent cells (stored at -80°C) were combined with 3µl of the ligation product and incubated on ice for 20 minutes. The competent cells were then heat shocked in a 42°C water bath for 1 minute and further put on ice for 5 minutes. 300µl of LB medium was added and 100 were transferred to LB plates containing ampicillin. The plates were incubated for 16 hours at 37°C.

## **2.4 Small Scale DNA Isolation (Mini Prep)**

Single colonies from LB plates were picked and incubated in 2ml LB medium supplemented with 50µg/ml ampicillin for 16 hours in a 37°C shaking incubator. Following small scale DNA isolation was performed using the QIAprep Spin Miniprep Kit (Qiagen), according to manufacturer's instructions. DNA concentration was determined using NanoDrop™ (Thermo Scientific).

## **2.5 Large Scale DNA Isolation (Maxi Prep)**

Either single colonies from LB plates were picked, or 30µl of an overnight mini prep culture was incubated in 500ml LB medium supplemented with 50µg/ml ampicillin for 16 hours in a 37°C shaking incubator. Subsequently, large scale plasmid isolation was performed using the Qiagen HiSpeed Plasmid Midi Kit (Qiagen). Some adjustments were made to the manufacturer's protocol after eluting the DNA with 5ml QF buffer: 3.5ml isopropyl alcohol (VWR) were added and incubated for 5 minutes. Thereafter the mixture was spun down at 10,000 rpm for 30 minutes. The supernatant was aspirated, the DNA was washed with 5ml 70% ethanol, and centrifuged for 10 minutes at 10,000 rpm. The supernatant was aspirated and the DNA pellet was allowed to dry at room temperature, until it looked transparent. Subsequently, the pellet was resuspended in 150-300 µl (depending on size) TE buffer, and incubated for 16 hours at RT to dissolve. The next day, the tube was spun down for 5 minutes at 10000 rpm and the supernatant was transferred to a new Eppendorf tube. DNA concentration was determined using NanoDrop™ (Thermo Scientific).

## **2.6 Maintenance/Propagation of HEK 293T Cells**

HEK 293T cells were grown in Dulbecco's Modification of Eagle's Medium with 4.5g/L glucose, L-glutamine & sodium pyruvate (DMEM) (Corning) supplemented with 10% HI FBS (Gibco) and 2% Penicillin Streptomycin solution (Corning), and passaged 1:10 on a 3-4-day schedule (at 90% confluency) using 0.25% Trypsin (Corning). 293T cells were maintained at 37°C and 5% CO<sub>2</sub>.

## 2.7 Transfection of HEK 293T Cells

293T cells were split in a 1:5 ratio from a 10cm plate to a 12-well plate. At 70-90% confluency, 0.25µg CRISPR gRNA plasmid (lentiGuide puro, plasmid #52963, Addgene) and 0.5µg pCas9-GFP (plasmid #44719, Addgene) were combined with 300µl serum free DMEM and 3µl PEI (3:1) and incubated for 20 minutes at room temperature. The mixture was then added dropwise to the cells.

## 2.8 Polymerase Chain Reaction (PCR) Amplification

Genomic DNA from transfected 293T cells was isolated using the gDNA Qiagen DNEasy kit (Qiagen) according to manufacturer's instructions. For PCR amplification Phusion Hot Start II High Fidelity DNA Polymerase (Thermo Scientific) was used, in the following master mix: 50-100ng DNA, 4µl Phusion buffer, 0.8µl primer 1 (1µM), 0.8µl primer 2 (1µM), 1.6µl dNTPs, 0.125µl Phusion Hot Start II High Fidelity DNA polymerase and H<sub>2</sub>O for a final volume of 20µl. Depending on the expected PCR product length, different cycling conditions were used:

### PCR amplification

<1000 base pairs

98	2min		
98	10s	}	X 40
60	15s		
72	20s		
72	1min		
16	hold		

>1000 base pairs

94	2min		
94	10s	}	X 40
55-65	20s		
72	1min		
72	1min		
16	hold		

## 2.9 Gel Electrophoresis

The PCR reactions were analyzed using a 2% agarose gel (<1000 bp), or a 1% agarose gel (>1000 bp). The agarose powder was dissolved in TBE buffer, and mixed with 0.001% GelRed™ (Biotium). The gel was run using a Biorad gel running

station filled with TBE buffer. For length determination, a 1kb plus ladder (Life Technologies) was used. The gel was analyzed with the Alphamager HP geldocumentation system (Protein Simple).

## **2.10 Gel Elution and Sequencing**

Gel elution was transformed using the QIAquick Gel Elution Kit (Qiagen) following manufacturer's instructions. The obtained DNA was submitted for sequencing to Genewiz following instructions on: <https://www.genewiz.com/>.

## **2.11 Maintenance/Propagation of HuES8 Cells**

The Human Embryonic Stem cell line 8 (HuES8) was cultured in Geltrex® (Life Technologies) matrix coated plates (1:100 in DMEM, coated for 1 hour), in mTeSR™1 (Stemcell Technologies), supplemented with 2% Penicillin Streptomycin solution (Corning) and 0.5µg/ml Plasmocin (Invivogen). Cells maintained at 37°C and 5% CO<sub>2</sub> and media was changed every 24 hours. HuES8 were passaged routinely at 80-95% confluency 1:10 on a 3-4-day schedule, using Accutase® Cell Detachment Solution (VWR) (1:4 in DPBS, Corning). For each passage, HuES8 were treated with 10µM ROCK inhibitor (Y-27632, Santa Cruz Biotechnology).

## **2.12 Electroporation of HuES8 Cells**

HuES8 were detached using 1:4 Accutase, and diluted in 700µl DPBS and mixed with 12.5µg of the respective CRISPR gRNA plasmids and 50µg pCas9-GFP. Cells were electroporated using the GenePulser Xcell™ (Biorad). Electroporated HuES8 were spun down at 1000rpm for 5 minutes and plated in a Geltrex coated plate in mTeSR supplemented with ROCK inhibitor, as stated above.

## **2.13 Determination of Genome Edited Cells**

Previously electroporated HuES8 were grown for 48 hours, detached using 1:4 Accutase, and diluted in 300µl DPBS and GFP positive cells were sorted out using BD

FACSAria II (BD Bioscience). GFP positive cells were plated on a Geltrex coated plate at single cell density in conditioned mTeSR (1:1 mixture of fresh mTeSR (supplemented with Penicillin Streptomycin solution and Plasmocin) and collected mTeSR). The conditioned mTeSR was additionally supplemented with ROCK inhibitor (for 14 hours) and 7ng/ml bFGF to suppress differentiation. After one week, single colonies were picked and further maintained in 96 well plates until 80-90% confluency.

## 2.14 Large Scale Screening for Knockout Clones

Confluent 96 well plates were split to obtain a replica maintenance plate and a plate used for genomic DNA isolation. Cells were spun down for 5 minutes at 1800 rpm and the remaining medium was poured off. Genomic DNA was extracted using prepGEM® Tissue Kit (ZyGEM), following manufacturer's instructions. 2µl of the extracted DNA were used for PCR amplification (see 2.8). Yet the cycling conditions were slightly different:

95	2min		
95	15s	}	X 40
58	15s		
72	15s		
72	2min		
16	hold		

PCR products were further analyzed using gel electrophoresis and selected knock-out clones were further maintained.

## 2.15 Differentiation of HuES8 into Endothelial Cells

For differentiation into Endothelial Cells (ECs), 2 different protocols were used:

### 2.15.1 Protocol 1

Differentiation into ECs was conducted as described in “Generation of vascular endothelial and smooth muscle cells from human pluripotent stem cells” by Challet-Meylan et al. <sup>28</sup>, including some adjustments.

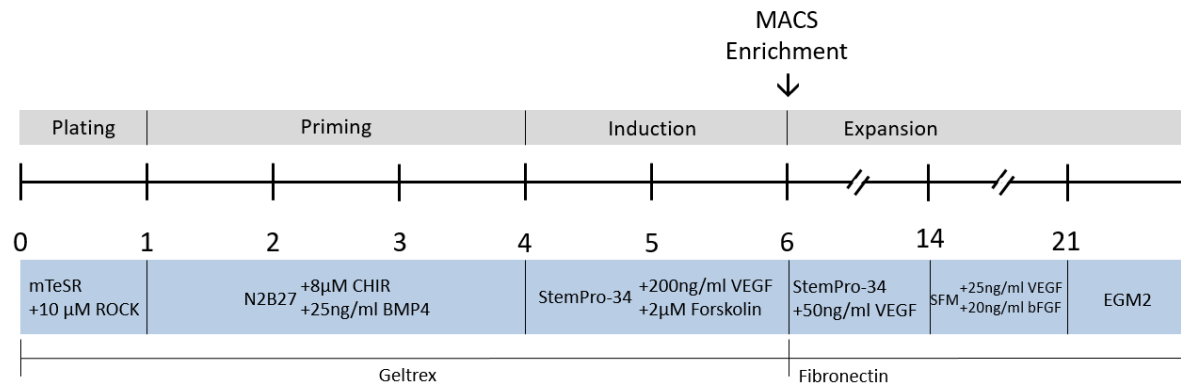


**Figure 5: Flow chart EC differentiation Protocol 1.**

This figure shows the flow chart of EC differentiation protocol 1, adapted from Challet-Meylan et al. <sup>28</sup>. The protocol takes 6 days to obtain CD144 and CD31 positive ECs. For further maturation the cells were kept in several maturation and differentiation media for 2 more weeks.

On day 0, 1.5 million HuES8 (wildtype and knockout clones) were seeded in a Geltrex coated T75 flask, in 50ml mTeSR supplemented with ROCK inhibitor, and incubated overnight at 37°C, 5% CO<sub>2</sub>. On day 1, the medium was replaced with N2B27 Medium (500ml DMEM/F12 (Gibco) + 500ml Neurobasal medium (Life Technologies) + 20ml Supplement B27 minus Vitamin A (Life Technologies) + 10ml N-2 Supplement (100X, Life Technologies) + 1ml 2-Mercaptoethanol (50mM, Life technologies), supplemented with 8 $\mu$ M CHIR-99021 (Cayman), and 25ng/ml BMP4 (R&D Systems) for 3 days, without media change. On day 4 and day 5, the medium was replaced with 40 ml StemPro-34 SFM (500ml StemPro-34 (Gibco) + 5ml Penicillin Streptomycin (1:100) + 5ml Glutamax (1:100, Life Technologies) + StemPro-34 Supplement) supplemented with 200ng/ml VEGF165 (VEGFA, Preprotech), and 2 $\mu$ M Forskolin (Abcam). On day 6, a MACS enrichment using CD144 MicroBeads (Miltenyi Biotec) was performed according to manufacturer’s instructions. The enriched ECs were plated on a fibronectin (VWR) coated plate in StemPro-34 SFM containing 50ng/ml VEGF, and medium was changed every other day. At 100% confluency,

the ECs were split 1:5 onto a fibronectin coated plate in Human Endothelial SFM (Life Technologies), with medium being changed every other day. At 100% confluency, the ECs were split 1:5 onto a fibronectin coated plate in Endothelial Cell Growth Medium supplemented with SingleQuots™ Kit (Lonza) and 2% Penicillin Streptomycin solution, with media change every other day. During the whole differentiation and expansion process the ECs were maintained at 37°C and 5% CO<sub>2</sub>.

### 2.15.2 Protocol 2

The second protocol was generated by combining two different protocols including: “Generation of vascular endothelial and smooth muscle cells from human pluripotent stem cells”<sup>28</sup>, and “Mapping the Pairwise Choices Leading from Pluripotency to Human Bone, Heart, and Other Mesoderm Cell Types” by Loh et al.<sup>29</sup>.

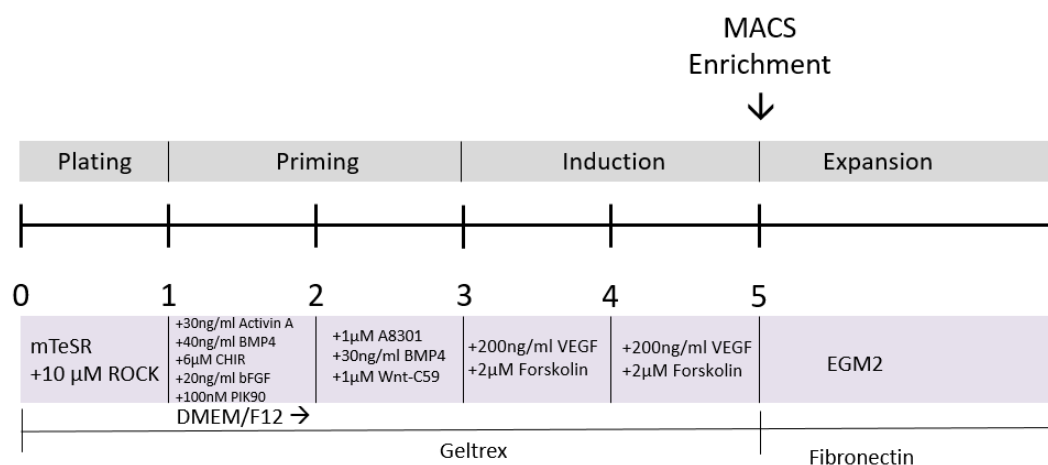


**Figure 6: Flow chart of EC differentiation Protocol 2.**

This figure shows a flow chart of EC differentiation protocol 2, adapted from Challet-Meylan et al.<sup>28</sup>, and Loh et al.<sup>29</sup>. The protocol takes 5 days to obtain CD144 and CD31 positive ECs. Since no further maturation of the ECs was needed, the cells were immediately taken for further assays.

200,000 HuES8 cells (wildtype and knockout) per well were seeded onto a Geltrex coated 6 well plate in mTeSR supplemented with ROCK inhibitor and incubated overnight. On day 1 the medium was changed to 2ml/well DMEM/F12 (+2% glutamine, 2% Penicillin Streptomycin solution) supplemented with 30ng/ml Activin A (Cell Guidance Systems), 40ng/ml BMP4, 6μM CHIR, 20ng/ml bFGF, and 100nM

PIK90 (Cayman). The following day the cells were fed with 2ml/well DMEM/F12 containing 1 $\mu$ M A8301 (Cayman), 30ng/ml BMP4, and 1 $\mu$ M Wnt-C59 (Cayman). On day 3 and 4 the medium was changed to DMEM/F12 supplemented with 200ng/ml VEGF and 2 $\mu$ M Forskolin. On day 5 the differentiated ECs from one 6 well plate were combined and enriched using the MACS CD144 MicroBeads (Miltenyi Biotec) following manufacturer's instructions. The enriched ECs were plated onto a Fibronectin coated plate in Endothelial Cell Growth Medium supplemented with Single-Quots™ Kit and 2% Penicillin Streptomycin solution. Media was changed every other day until cells were used for assays. During the whole differentiation and expansion process the ECs were maintained at 37°C and 5% CO<sub>2</sub>.

## **2.16 Flow Cytometry Staining and Analysis**

Depending on cell density between 200,000 and 1 million cells were harvested, washed with DPBS, and blocked in 4% FBS/DPBS for 30 minutes. The cells were further stained for 45 minutes in 1% FBS/DPBS with corresponding, stated antibodies (see Annex). Flow Cytometry was performed with either FACS Calibur™ or LSRII (BD Bioscience). Thereafter, FlowJo software (TreeStar) was used for analysis.

## **2.17 Poly(I:C) Treatment of Endothelial Cells**

Per clone, 500,000 cells per well (6 well plate, 3 wells per clone) were seeded onto Fibronectin in 2ml/well Endothelial Cell Growth Medium supplemented with Single-Quots™ Kit and 2% Penicillin Streptomycin solution, and incubated at 37°C and 5%CO<sub>2</sub> for 16 hours. The following day the cells were treated with poly(I:C) in 2 different ways. The first was by using the Lipofectamine™ 3000 Reagent Protocol (Thermo Scientific) following manufacturer's instructions. The second one was by directly adding poly(I:C) combined with serum free DMEM dropwise to the cells. Also 1 well per clone was not treated, to serve as a negative control. The cells were further incubated for 6-12 hours (RNA isolation) and 18 hours (Western Blot) at 37°C and 5% CO<sub>2</sub>.

## 2.18 RNA Isolation

RNA isolation was conducted by using the TRIzol™ Reagent following manufacturer's instructions. RNA concentration was determined using NanoDrop™.

## 2.19 cDNA Synthesis

For cDNA synthesis qScript™ cDNA SuperMix (Quanta Biosciences) was used according to manufacturer's instructions. The reaction was assembled by using 1µg RNA in 16µl H<sub>2</sub>O and 4µl qScript cDNA SuperMix (5X). Yet, amendments of the cycling conditions were made:

### cDNA synthesis

25	5min
42	1h
85	5min
4	hold

Thereafter, the cDNA was diluted with 80µl H<sub>2</sub>O.

## 2.20 Quantitative Real Time PCR

2µl of diluted cDNA were combined with 5µl SYBR® green (Life Technologies), 1.5µl primer mix (10µM each), and 1.5µl H<sub>2</sub>O. Quantitative PCR was run on ViiA 7 (ThermoScientific), and relative expression was determined with Excel (Microsoft).

## 2.21 Western Blot

Poly(I:C) treated cells were lysed with lysis buffer containing: 10X RIPA Lysis and Extraction Buffer (ThermoScientific), 1X PMSF (Cell Signaling Technologies), 1mM Dithiothreitol (Sigma Aldrich), and H<sub>2</sub>O, to obtain the final volume. NuPAGE® LDS Sample Buffer (4X, Life Technologies) was added, and the sample was incubated for 7 minutes at 95°C. The samples were loaded into NuPAGE® 4-12% Bis-Tris Gel (Life Technologies) in NuPAGE® MOPS SDS Running Buffer (Life Technologies).

Thereafter the samples were blotted onto Nitrocellulose/Filter Paper Sandwiches 0.45 $\mu$ M (BioRad) at 90V, for 2 hours at 4°C. The membrane was furthermore blocked for 1 hour in 5% BSA (VWR) in TBST, and stained for 16 hours with the primary antibodies at 4°C. Thereafter the membrane was washed and stained with the secondary antibodies for 1 hour at room temperature. After further washing steps the membrane was developed using a 1:1 combination of LumiGlo® Reagent A (20X) and Peroxide Reagent B (20X, Cell Signaling Technologies) on the Fluor-Chem M chemiluminescence Imager (Protein Simple).

## **2.22 Statistical Analysis**

Data are expressed as mean values  $\pm$  standard deviation and results were evaluated by Student's two-tailed t test.  $p < 0.05$  was considered statistically significant. In all figures, \* $p < 0.05$ , \*\* $p < 0.01$ , and \*\*\* $p < 0.001$ .

---

## 3 Results

### 3.1 Specific Deletion of *IFIH1* Start Codon

To test our hypothesis whether *IFIH1* knockout would prevent T1D disease related cells from overshooting stress response, we decided to delete the *IFIH1* gene (location 2q24.2) using CRISPR-Cas9. We therefore chose to target the start codon in exon 1. A dual guide strategy was designed to specifically remove the interval between the gRNAs<sup>30</sup>, in this case spanning the start codon. Four different gRNAs (sequences listed in Supplemental Table 1) were cloned and tested in different combinations in HEK 293T cells to determine cutting efficacy. Cutting, and the subsequent selection of clones was determined by PCR screening. A set of primers (TB009+TB010, sequences listed in Supplemental Table 2) were designed to span the region of the desired CRISPR cutting. A schematic representation of the *IFIH1* targeting strategy can be seen in Figure 7A below. The wildtype (WT) PCR band, as in the untreated cells, and clones, where no CRISPR cutting occurred was 356 base pairs of length, whereas the knockout (KO) band was expected to be 197 base pairs long. All expected PCR band lengths are summarized in Figure 7B below. PCR and gel electrophoresis analysis of transfected 293T cells show no cutting efficiency when using CRISPR gRNA combinations 1+3, 2+3, and 2+4 occurred. However, combination 1+4 lead to sufficient cutting (see Figure 7C). Hence, CRISPR gRNA combination 1+4 was used for genome editing of HuES8 stem cells.

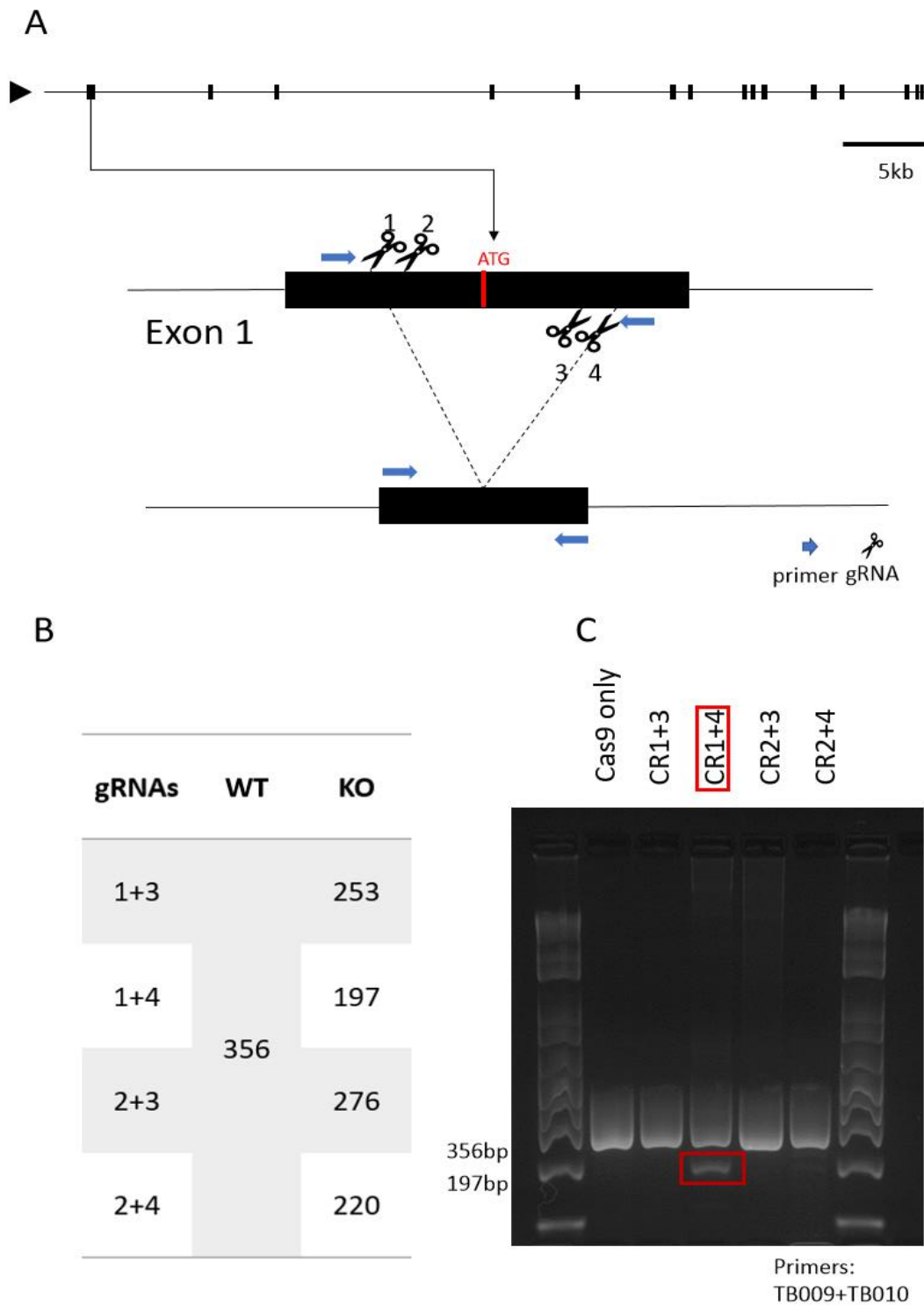


**Figure 7: IFIH1 targeting strategy.**

A) Schematic representation of IFIH1 gene to visualize targeting strategy to specifically delete the start codon in exon 1, highlighted in red. Primers used for PCR amplification are indicated as blue arrows; B) Table summarizing all expected PCR band lengths of different CRISPR gRNA combinations; C) PCR analysis of 293T cells transfected with different gRNA combinations show efficient CRISPR on-target activity in combination 1+4.

Subsequently, HuES8 were electroporated with the selected CRISPR gRNAs combination 1+4 and pCas9\_GFP, to delete the *IFIH1* start codon. Electroporation efficiency was analyzed by GFP expression of pCas9\_GFP, which was checked 24 hours post-electroporation under a fluorescence microscope. As expected, the negative control (non-electroporated) showed no GFP expression, whereas GFP was expressed in electroporated cells after 24 hours (see Figure 8A). 48 hours after electroporation, electroporated GFP positive cells were sorted out using FACS, assuming cells that took up pCas9\_GFP, also took up the CRISPR gRNAs, and the start codon was deleted (see Figure 8B). The GFP positive cells were re-plated and grown in single cell density until colonies were large enough to be manually picked and split into a well of a 96-well plate each. Subsequent large scale PCR screening of single cell derived clones demonstrated several homozygous *IFIH1* KO clones, as indicated by the presence of the KO PCR band and lack of the WT band (see Figure 8C). DNA sequencing confirmed the deletion of the start codon in clone B6/P2 (see Figure 8D), further referred to as *IFIH1* “KO” clone.



### 3.2 Successful Differentiation and Enrichment of HuES8 Derived Endothelial Cells

After the creation of an *IFIH1* KO cell line, the cells had to be differentiated into T1D related cells, such as pancreatic beta cells and Endothelial Cells (ECs) for further assays. We decided to start with an EC differentiation, since they are also T1D related cells, as they are also found in the pancreatic islets<sup>31</sup>. Furthermore, the EC differentiation protocols are rather short and comparably easy. To exclude variability in genetic background, parental HuES8 and KO cell lines were differentiated into ECs side by side, as isogenic cell lines, following protocol 1 (see 2.15.1). Differentiation, as stated in the protocol, took 6 days. After completed differentiation it is of major importance to sort or enrich the differentiated ECs, to eliminate undifferentiated cells and ensure reliable and reproducible further results. Enrichment of ECs was obtained by using MACS and CD144-conjugated magnetic beads. CD144 is also called VE-cadherin, and together with CD31 represents cell surface markers of ECs.<sup>32</sup> Pre- and post- enrichment samples were stained with anti-CD31 antibody to determine differentiation and enrichment efficiency. It is important to stain with another antibody – different than CD144 – for flow cytometry because the probability that CD144 will still be blocked by the magnetic beads after enrichment is very high. Hence it is crucial to use CD31 antibody, to obtain reasonable enrichment efficiency analysis. CD31 positive and negative cells were gated out of the live cell population (Figure 9A). By flow cytometry analysis of CD31 negative and positive cells pre- and post-enrichment, enrichment efficiency was determined. Visible enrichment in CD31 positive cells after MACS sort can be observed, and furthermore enrichment efficiency was consistent for both WT and KO cells (see **Figure 9**Figure 9B+C). On the contrary, mean fluorescence intensity (MFI) did not differ between the KO and WT cells (Figure 9D). The determined fold enrichment of CD31 positive WT and KO cells was 1.2 and 1.4 respectively.

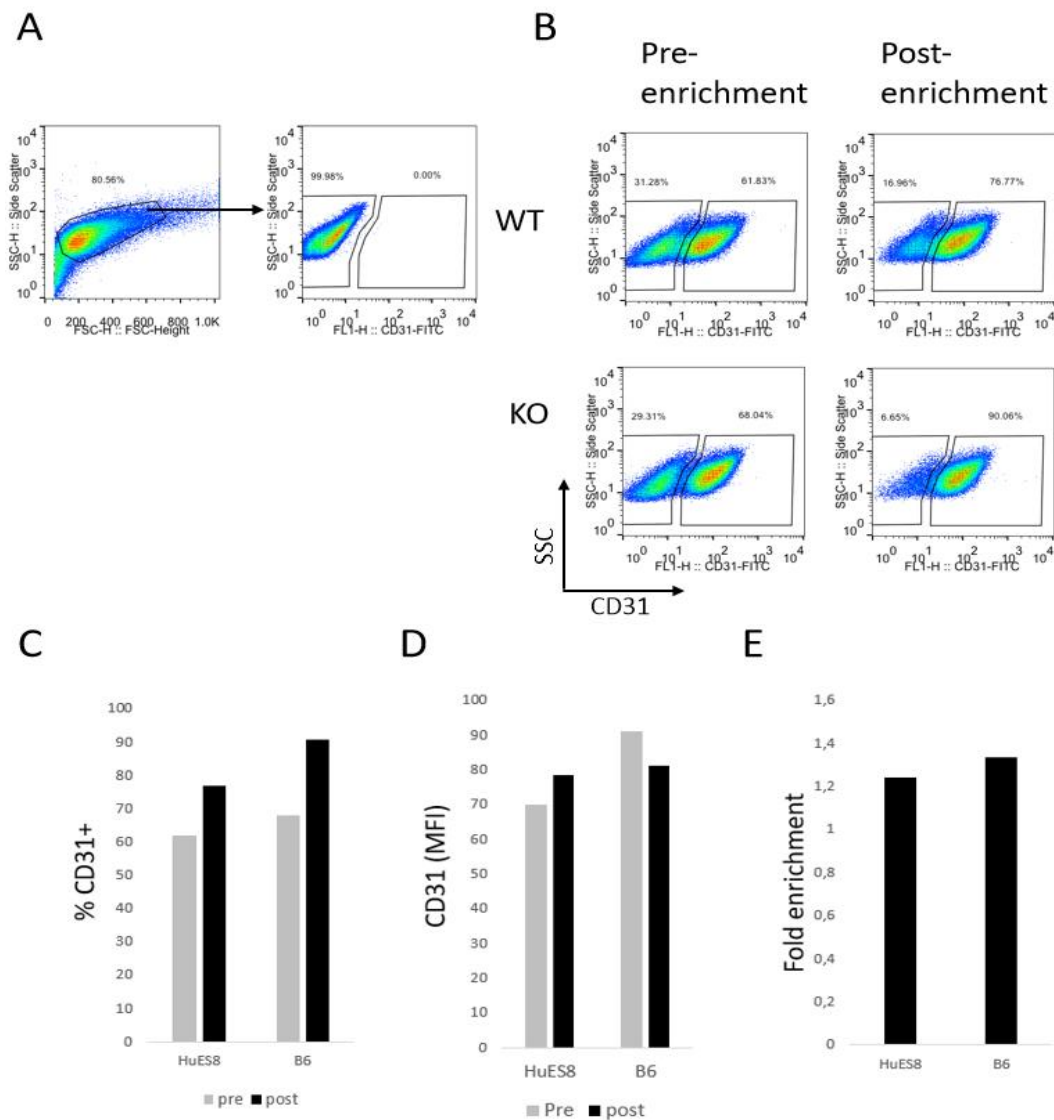


**Figure 9: Flow Cytometry analysis of MACS enriched ECs (protocol 1).**

A) Gating strategy: CD31 negative (left gate in 2<sup>nd</sup> plot), and CD31 positive (right gate in 2<sup>nd</sup> plot) were gated out of the live cell population (gate in 1<sup>st</sup> plot); B) Pre- and post-enrichment CD31 populations of WT and KO cell lines, with visible successful enrichment; C) Percentages of CD31+ cells pre- and post-enrichment of WT and KO cells; D) Mean Fluorescence Intensity (MFI) of CD31+ pre- and post-enrichment WT and KO cells; E) Fold enrichment of WT and KO cell lines.

### 3.3 qPCR and Western Blot Reveal Residual *IFIH1* mRNA and MDA5 Protein Expression

As we hypothesized that *IFIH1* KO would reduce a high immune response upon viral infection, we decided to mimic viral infection by stimulating the cells with synthetic dsRNA (poly(I:C)). The isogenic HuES8 derived ECs were treated with 10 µg/ml poly(I:C), by either lipofecting the cells, or by just adding the reagent to the medium. For each experiment, also a negative control (non-treated cells) was done. For determination of *IFIH1* mRNA levels, cells were treated with poly(I:C) for 6 hours, whereas they were stimulated for 18 hours for determination of MDA5 expression on the protein level. After treatment WT and KO ECs were harvested for either qPCR or Western blot. All “treated” data below indicates lipofected poly(I:C) (poly(I:C) just added to the medium data not shown). First, RNA isolation and subsequent cDNA synthesis were performed to determine mRNA levels: Interestingly, there was no reduction in *IFIH1* mRNA expression in the KO cells (Figure 10A), however a slight decrease in IFN $\beta$ , a target gene in the MDA5 signaling pathway (compare **Figure 44**), expression was observed in the KO cells. To confirm these findings, a Western blot for MDA5 was performed (Figure 10B). Indeed, MDA5 protein was detected in both WT and KO cell lines after 18 hours poly(I:C) treatment, indicating that there is still residual functional MDA5 present in the *IFIH1* KO cell line. These findings are contradictory to the data above, where DNA sequencing confirmed deletion of the *IFIH1* start codon. We interpreted these findings as the generation of a truncated, but still functional MDA5 protein, due to exon skipping and an alternative start codon. This assumption can be further confirmed by precise analysis of the Western blot, as the KO MDA5 appears to be slightly reduced in length, when compared to the WT protein.

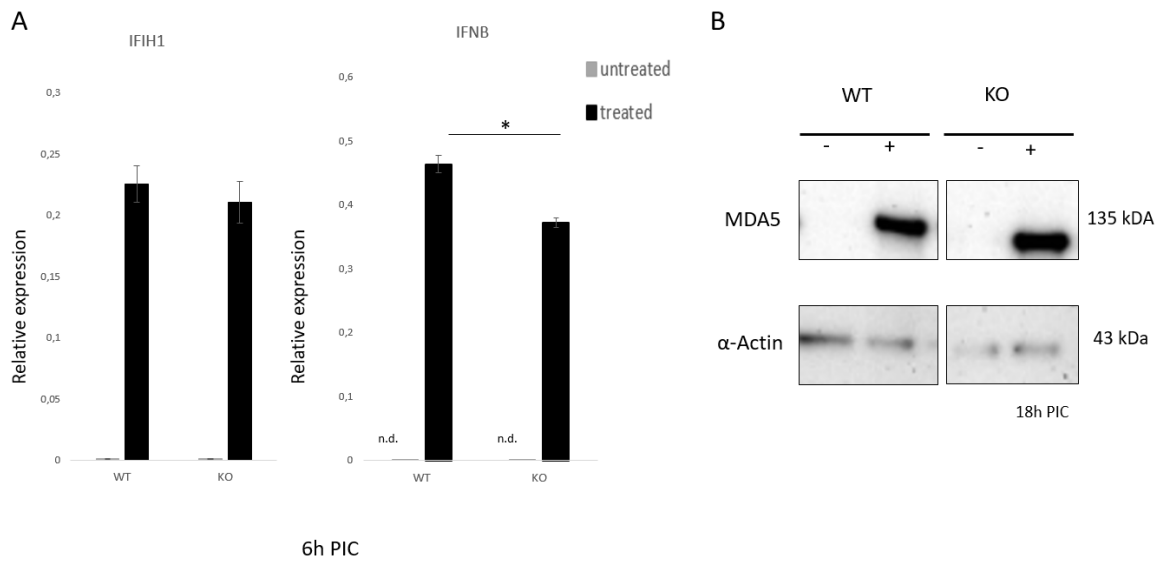


**Figure 10: Determination of *IFIH1* and *IFNβ* expression in WT and KO ECs.**

A) qPCR to determine *IFIH1* and *IFNβ* mRNA expression in WT and KO cells after 6 hours poly(I:C) treatment; B) Western blot to analyze MDA5 protein expression in WT and KO cells after 18 hours poly(I:C) treatment; “treated” indicates lipofected with 10 μg/ml poly(I:C).

### 3.4 Revised *IFIH1* Targeting Approach

As there was still residual, truncated, but nevertheless functional MDA5 present in the KO cell line, we decided to revise our *IFIH1* targeting approach and to delete the entire gene (Figure 11A), to prevent exon skipping and subsequent truncated protein expression. Four new CRISPR gRNAs located at the far end of the *IFIH1* gene were designed, cloned and tested in combination with gRNAs 1 and 4 from the previous targeting strategy. Additionally, a new reverse primer (TB0053) was designed to determine *IFIH1* KO in combination with the previously used primer TB009. Due to the length of the *IFIH1* gene (>50,000 base pairs), the new primer pair (TB009+TB053) would only be able to amplify a PCR product, if CRISPR/Cas9 cut out the gene, resulting in a 526 base pair long fragment, otherwise the piece would be too big to amplify with the used PCR cycling conditions. All newly designed CRISPR gRNAs and the expected PCR band lengths, are summarized in Figure 11B. Before electroporating HuES8, the new CRISPR gRNAs were tested in 293T cells. CRISPR gRNA combination 4+12 was most efficient in on-target activity and cutting efficiency (Figure 11C), compared to the other gRNA combinations (not

shown). The first lane on the agarose gel (Figure 11C) shows amplification of a WT PCR band (356 base pairs), when using the old primer combination, whereas in the second lane, one can see a PCR band of approximately 500 base pairs of length, when using the new primer pair, indicating successful CRISPR/Cas9 cutting. The CRISPR gRNA combination further used for electroporation of HuES8 was 4+12, since on-target activity was determined in 293T cells. As explained in 3.1 above, HuES8 were electroporated with the selected gRNA combination and pCas9\_GFP. 24 hours post electroporation, GFP expression was checked under the fluorescence microscope and after 48 hours the GFP positive cells were sorted out using FACS and re-plated in single cell density. Genomic DNA of the single cell derived clones was extracted for large scale PCR screening. 4 *IFIH1* KOs were identified as *IFIH1* KOs (Figure 11D). DNA of identified KO clones was submitted for sequencing and sequence of clone D2, further referred to as “KO”, confirmed deletion of the entire *IFIH1* gene (Figure 11E).

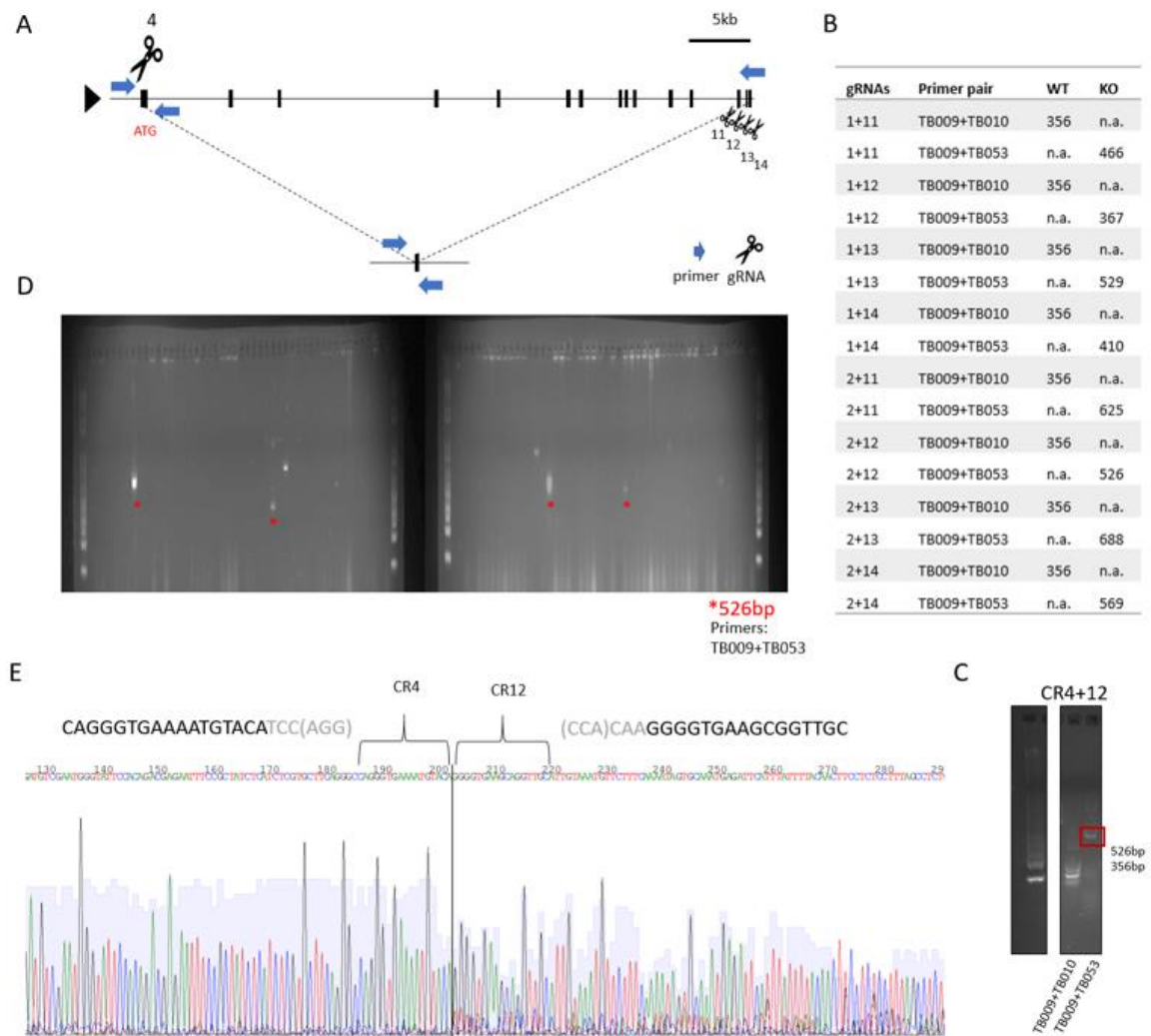


**Figure 11: Deletion of entire IFIH1 gene by revised targeting approach.**

A) Schematic representation of IFIH1 gene to visualize the new targeting strategy, aiming to delete the entire gene; B) Summary of all designed and tested CRISPR gRNAs and the expected PCR band lengths; C) PCR analysis of 293T cells transfected with gRNA combination 4+12 show efficient CRISPR/Cas9 cutting efficiency; D) PCR and gel electrophoresis analysis of gDNA of electroporated HuES8 show 4 IFIH1 KOs (\*); E) Sequence confirmation of precise IFIH1 deletion in KO clone.

After identification of an *IFIH1* KO clone, cells were again differentiated side by side with parental HuES8 into ECs, using a new protocol (see 2.15.2). Protocol 2 uses small molecules, instead of growth factors to achieve differentiation of stem cells into ECs, which subsequently makes it much more robust and reproducible. Also, it only takes 5 days (in comparison with protocol 1, which takes 6 days). Nevertheless, after completed differentiation, the ECs have to be enriched, which was performed using MACS and CD144 magnetic beads. Pre- and post-enrichment samples were stained with anti-CD31 antibody and analyzed by flow cytometry to identify differentiation and enrichment efficiency. CD31 positive and negative cells were gated out of the live cell population (Figure 12A), and further analysis presented visible CD31 positive cell enrichment after MACS sort (Figure 12B), which was further confirmed by percentages of CD31 positive cells pre- and post-enrichment (Figure 12C), and MFI values (Figure 12D). When using protocol 2 there was a WT and KO cells fold enrichment of 1.8 and 3.7 respectively (Figure 12E). When comparing protocol 2 to the previously used protocol 1, differentiation, as well as enrichment efficiency are noticeably higher in protocol 2.

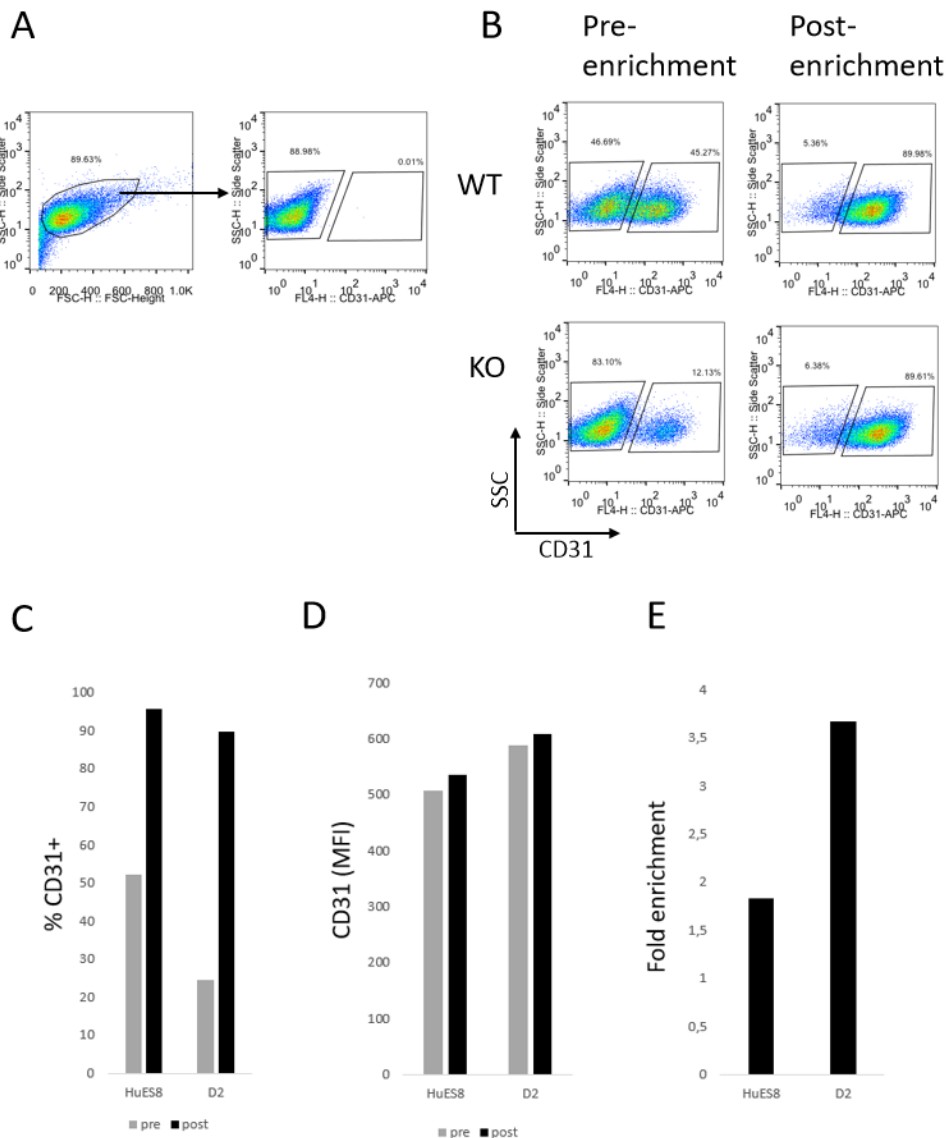


**Figure 12: Flow cytometry analysis of MACS enriched ECs (protocol 2).**

A) Gating strategy of CD31 negative and positive ECs out of the live cell population; B) Pre- and post-enrichment of WT and KO ECs; C) Percentages of WT and KO cell lines pre- and post-CD144 enrichment; D) MFI of WT and KO cells pre- and post-enrichment; E) Fold enrichment of KO and WT cell lines; with this figure it is possible to compare protocol 2 to protocol 1.

As explained in 3.3, the WT and KO cell lines were treated with poly(I:C) for 6 hours to mimic viral infection. Again, cells were lipofected with 10 $\mu$ g/ml poly(I:C) (data shown), and poly(I:C) was added to another set of cells (data not shown). After treatment, cells were harvested for qPCR, to determine *IFIH1*, and several target genes' mRNA levels (Figure 13). Although no difference in *IFIH1* expression in WT

and KO cells was observed, there is a significant decrease in IFN $\beta$  expression in KO cells after poly(I:C) treatment. Moreover, there is a significant decrease in IP10 mRNA levels in KO cells. On the contrary, increased levels of TNF and OAS levels in the KO cells were detected. No difference in mRNA levels between WT and KO cells were found for the genes IL6 and IL8.

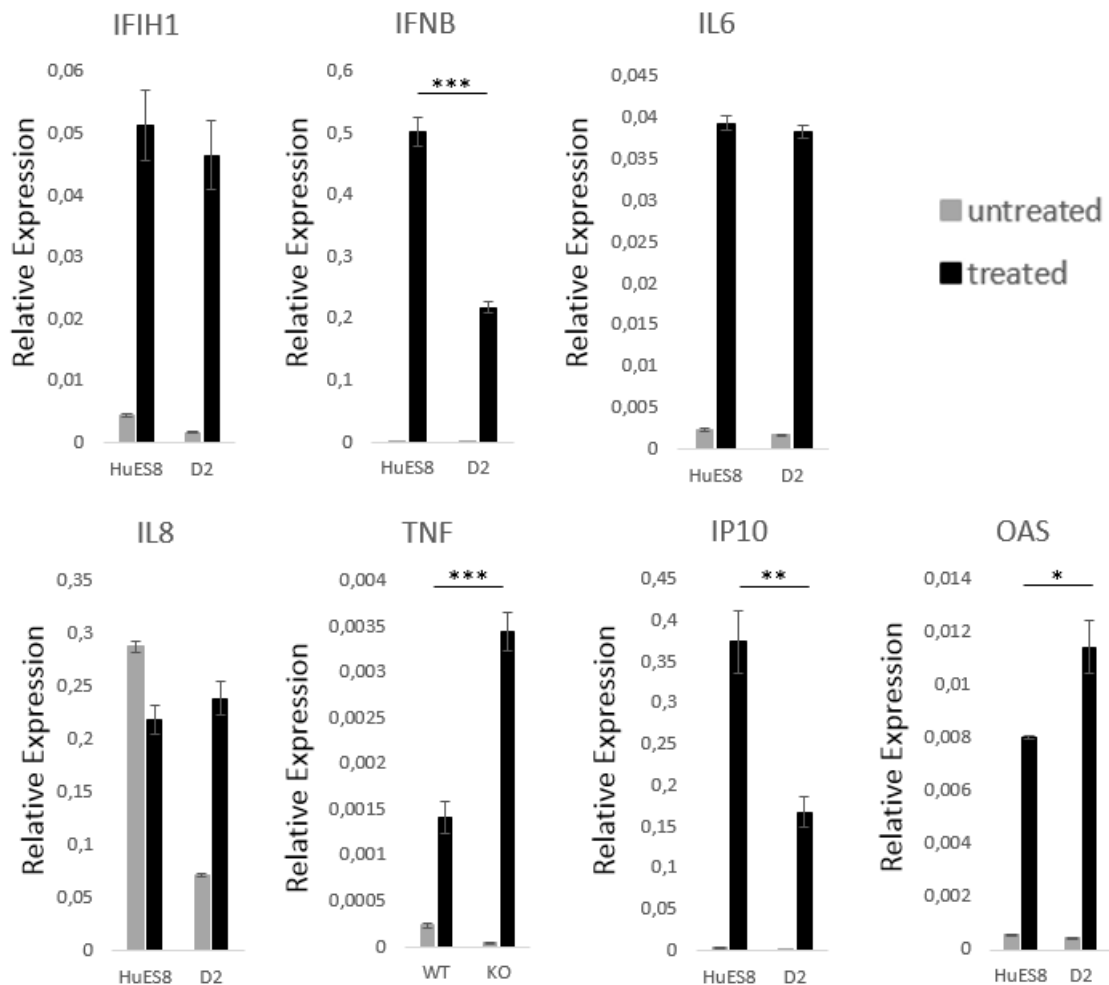


**Figure 13: qPCR to determine mRNA levels after mimicking viral infection;** mRNA expression of IFIH1 and several genes downstream of MDA5 signaling were determined: IFN $\beta$ , IL-6, IL-8, TNF $\alpha$ , IP10, and OAS.

## 4 Discussion

Several publications propose that *IFIH1* and its encoded protein MDA5 play a crucial role in sensing cytoplasmic dsRNA, and in T1D development<sup>15,33-35</sup>. Different SNPs in the *IFIH1* locus have been identified to be rare protective variants against T1D<sup>36</sup>. Four of the latter result in either a truncated protein, alternative splicing, or amino acid exchanges<sup>33</sup>. Further studies demonstrated that reduction of MDA5 in MDA5<sup>+/-</sup> mice is protective against T1D onset, compared to MDA5<sup>-/-</sup> mice, which were completely protected from the disease, and MDA5<sup>+/+</sup> mice<sup>15</sup>.

Since all these studies have been conducted in mice, we wanted to investigate the result of *IFIH1* KO in human stem cell derived disease relevant cells, such as ECs and pancreatic  $\beta$  cells, to generate a disease model for further investigation of the role of *IFIH1* in T1D. We hypothesized that *IFIH1* KO would protect cells from overshooting immune response after viral infection, and might therefore protect from T1D onset. Consequently, our first approach was to delete the *IFIH1* gene, and subsequently MDA5 expression, by targeting the start codon in exon 1, with the assumption: no start codon, no protein. We successfully generated *IFIH1* KO cell lines (confirmed by DNA sequence and gel electrophoresis analysis), nevertheless, mimicking viral infection with poly(I:C) treatment showed no reduction in *IFIH1* mRNA levels (Figure 10A). From this result we concluded, that the mRNA might not have been degraded, hence Western blot was performed to confirm *IFIH1* KO on the protein level (Figure 10B). Interestingly, there was residual MDA5 protein expression in the KO cells, but qPCR analysis of one target gene, IFN $\beta$ , revealed significant mRNA reduction. We concluded, that a truncated, but still functional, although with slightly reduced activity, protein was generated by deleting the start codon in exon 1, most likely due to the use of an alternative start codon. This assumption was confirmed when looking at the protein structure (Figure 14). Wu et al. found that all MDA5 domains (Figure 14A) are important for dsRNA recognition, and the carboxy-terminal domain (CTD) is needed to recognize the internal duplex structure of dsRNA. Furthermore, the CTD docks to the helicase 2i (Hel2i) domain, and the helicase 2 (Hel2) domain is important for ATP hydrolysis<sup>35</sup>. It has been reported before, that MDA5 forms filaments upon dsRNA binding<sup>37</sup>, and thereby bringing 2 adjacent

helicase domains in close proximity, thereby leading to an extensive protein:protein contact, which explains MDA5's high affinity for dsRNA<sup>35</sup>. Whereas all domains seem to be crucial for dsRNA binding, Wu et al. proposed that only one domain, the 2CARD, at the N-terminal region of the protein might be important for binding the first downstream regulator MAVS (compare Figure 4). They confirmed their assumptions and created a model (Figure 14D), in which 2CARD forms discrete patches of oligomers along the MDA5 filament. Furthermore, 2CARD oligomerization (induced by ATP hydrolysis) is crucial to promote MAVS filament formation, and subsequent signal transduction<sup>35</sup>. These findings can be applied when analyzing the *IFIH1* start codon targeting approach. Since there is still residual MDA5 protein expressed upon dsRNA treatment in KO cells, the first exon (harboring the start codon) was most probably skipped, resulting in a truncated, functional protein. Exon 1 would therefore code in a region in the 2CARD domain, maybe leading to minor changes, that still enable oligomerization and association with MAVS, hence at a lower affinity than the WT MDA5, thereby explaining the minor reduction in IFN $\beta$  mRNA levels.

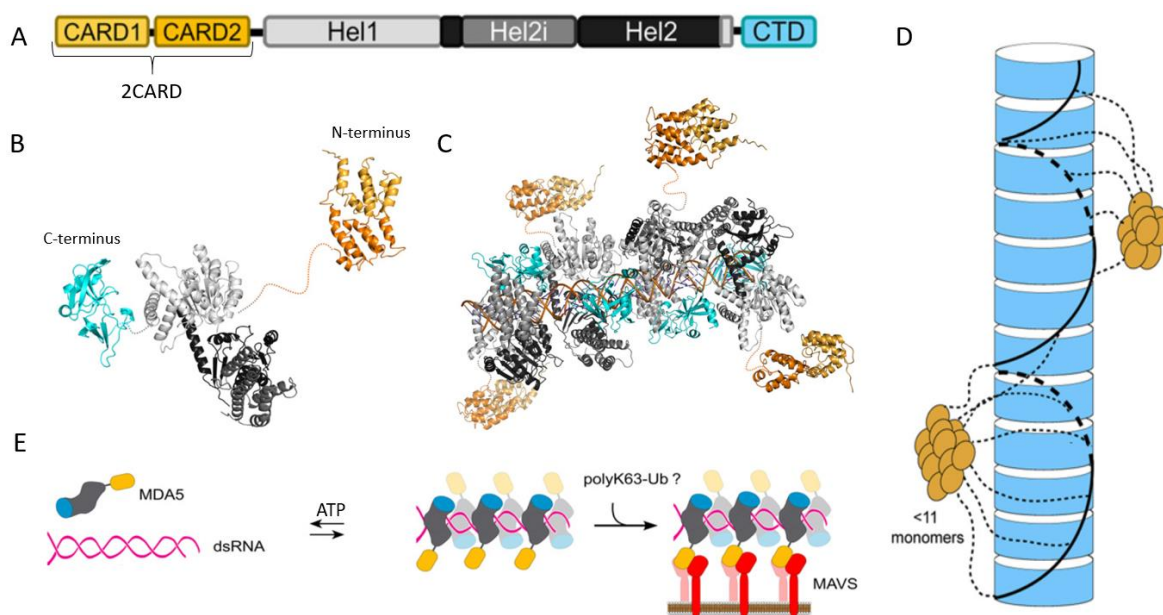


**Figure 14: Structural considerations of MDA5.**

A) Domain organization of MDA5: MDA5 consists of 2 CARD domains (CARD1 and 2), 3 helicase domains (Hel1, Hel2i, and Hel2), and a carboxy-terminal (CTD) domain; B) Open and loose conformation of MDA5 in absence of dsRNA; C) MDA5 forms head-to-tail filaments upon dsRNA binding; D) Model of 2CARD patch formation along MDA5 filaments, as proposed by Wu et al.; E) Binding of dsRNA results in MDA5 filament formation and subsequent 2CARD oligomerization by ATP hydrolysis enables association with mitochondrial membrane bound MAVS; modified from<sup>35,38</sup>.

Our second attempt to delete *IFIH1* was by targeting the entire gene. Again, *IFIH1* KO was confirmed by DNA sequencing and gel electrophoresis analysis. Unfortunately, we were not able to further confirm homozygosity due to contaminations in either PCR reagents, or primer dilutions or stocks. Therefore, we awaited qPCR results for determination of hetero- or homozygous KOs. Due to the fact, that there was no reduction in *IFIH1* mRNA levels, we concluded that *IFIH1* has only been deleted in 1 allele, but since patients carrying rare protective *IFIH1* variants are also heterozygous<sup>15</sup>, MDA5<sup>+/-</sup> KOs were considered as more relevant in establishing an actual disease model. Unfortunately, due to time constraints, it was not possible to check MDA5 expression on the protein level, but we hypothesized that protein expression in heterozygous KOs would be reduced, just as Lincez et al. showed in heterozygous mice<sup>15</sup>. Although there was no reduction in *IFIH1* mRNA levels detectable, there was a significant reduction of IFN $\beta$ , and IP10 (Interferon gamma-

induced protein 10), which has been shown to be upregulated in poly(I:C) treated cells<sup>39</sup>. Reduction of both IFN $\beta$ , and IP10 indicated decreased inflammatory response upon viral challenge. On the other hand, TNF $\alpha$ , and OAS, two proteins upregulated upon inflammation, are higher expressed in KO cells compared to the WT, which is contradictory to the reduction in IFN $\beta$  and IP10. One possibility for the elevated expression of TNF $\alpha$ , and OAS in KO cells might be the hyperactivation of TLR3 signaling pathway. TLR 3 is another viral sensor, and also leads to the upregulation of pro-inflammatory cytokines and interferons<sup>36</sup>.

Future directions for this study would be the repetition of assays to confirm the findings. Also, it would be of great importance to repeat the assays on stem cell derived  $\beta$ -cells, since they are affected cells in T1D. Furthermore, it would be helpful to determine the exact contribution of TLR3 signaling in *IFIH1/TLR3* double KO cell lines.

Conclusively it could be said that there is still a lot unknown about the role of *IFIH1* in T1D and its development. Nevertheless, *IFIH1* and its encoded protein MDA5 seem to be major players in disease development in genetically susceptible people upon viral infection. Therefore, MDA5 represents an important target for both preventive and therapeutic strategies to halt T1D.

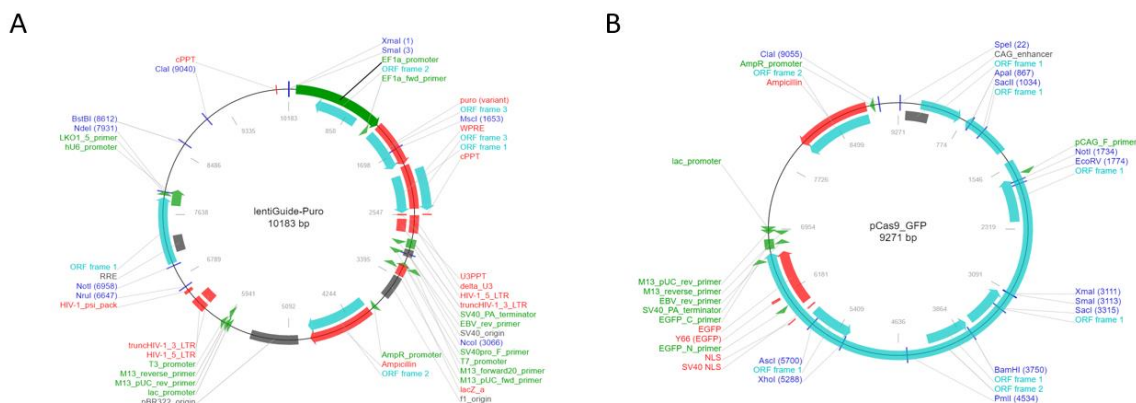
## List of References

1. Prevention CfDca. National Diabetes Statistics Report: Estimates of Diabetes and Its Burden in the United States. 2014.<http://www.cdc.gov/diabetes/pubs/statsreport14/national-diabetes-report-web.pdf>
2. Alejandro EU, Gregg B, Balandino-Rosano M, Cras-Méneur C, Bernal-Mizrachi E. Natural history of  $\beta$ -cell adaption and failure in type 2 diabetes. *Mol Aspects Med.* 2015 April:19-41.
3. Van Belle TL, Coppieters KT, Von Herrath MG. Type 1 Diabetes: Etiology, Immunology, and Therapeutic Strategies. *Physiological Reviews* 2011:79-118.
4. Jdrf. 2017 Type 1 Diabetes Facts. <<http://www.jdrf.org/about/fact-sheets/type-1-diabetes-facts/>>.
5. Floyel T, Kaur S, Pociot F. Genes Affecting Beta-Cell Function in Type 1 Diabetes. *Curr Diab Rep.* 2015 November:15(11):97.
6. Wallberg M, Cooke A. Immune mechanisms in type 1 diabetes. *Trends in Immunology* 2013 December.
7. Achenbach P, Bonifacio E, Kerstin K, Ziegler AG. Natural History of Type 1 Diabetes. *Diabetes* 2005 December:25-31.
8. Aggarwal I. The Epidemiology, Pathogenesis, and Treatment of Type 1 Diabetes Mellitus. *Inquiries Journal/Student Pulse* 2015.
9. Atkinson MA. The Pathogenesis and Natrual History of Type 1 Diabetes. *Cold Spring Harb Perspect Med* 2012.
10. Santamaria P. The Long and Winding Road to Understanding and Conquering Type 1 Diabetes. *Immunity* 32 2010 April 23.
11. Petzold A, Solimena M, Knoch K-P. Mechanisms of Beta Cell Dysfunction Associated With Viral Infection. *Curr Diab Rep* 2015 August 15.
12. Morgan NG, Richardson SJ. Enteroviruses as causative agents in type 1 diabetes: loose ends or lost cause? *Trends in Endocrinology and Metabolism* 2014 December.
13. Hober D, Alidjinou EK. Enteroviral pathogenesis of type 1 diabetes: queries and answers. *Curr Opin Infect Dis* 2013:263-269.
14. Bakay M, Padney R, Hakonsarson H. Comparative Geneti Analysis of Type 1 Diabetes and Inflammatory Bowel Disease. *Type 1 Diabetes - Pathogenesis, Genetics and Immunotherapy* 2011.
15. Lincez PJ, Shanina I, Horwitz MS. Reduced Expression of the MDA5 Gene IFIH1 Prevents Autoimmune Diabetes. *Diabetes* 2015 June:64(6):2184-93.
16. Looney BM, Xia C-Q, Concannon P, Ostrov DA, Clare-Salzler MJ. Effects of Type 1 Diabetes-Associated IFIH1 Polymorphisms on MDA5 Function and Expression. *Curr Diab Rep* 2015.
17. Hober D, Sauter P. Pathogenesis of type 1 diabetes mellitus: interplay between enterovirus and host. *Nature Reviews Endocrinology* 2010 May:279-289.
18. American Diabetes Association. 2014.
19. Mayo Clinic. Disease and Conditions - Type 1 Diabetes2014.

20. diaTribe. 2015 10/10. diaTribe. <<https://diatribe.org/google-secures-patent-glucose-sensing-contact-lens>>. Accessed 2016 10/10.
21. Pancreas and Islet Transplantation in Type 1 Diabetes. *Diabetes Care* 2006 April;935.
22. Sutherland RPR, Connie D, Jennifer L, Robert S, E.R DA. Pancreas and Islet Transplantation for Patients With Diabetes. *Diabetes Care* 2016;23:112-116<http://journal.diabetes.org/clinicaldiabetes/V18N42000/pg172.htm>
23. Hsu PD, Lander ES, Zhang F. Development and applications of CRISPR-Cas9 for genome engineering. *Cell* 2014;157(6):1262-78.10.1016/j.cell.2014.05.010.<https://www.ncbi.nlm.nih.gov/pubmed/24906146>
24. Wright AV, Nunez JK, Doudna JA. Biology and Applications of CRISPR Systems: Harnessing Nature's Toolbox for Genome Engineering. *Cell* 2016;164(1-2):29-44.10.1016/j.cell.2015.12.035.<https://www.ncbi.nlm.nih.gov/pubmed/26771484>
25. Kim H, Kim J-S. A guide to genome engineering with programmable nucleases. *Nature Reviews Genetics* 2014 May;321-334.
26. Perkel JM. 2016 October. Genome Editing with CRISPRs, TALENs and ZFNs. *Biocompare* <<http://www.biocompare.com/Editorial-Articles/144186-Genome-Editing-with-CRISPRs-TALENs-and-ZFNs/>>. Accessed 2016 October.
27. Seth RB, Sun L, Ea C-K, Chen ZJ. Identification and Characterization of MAVS, a Mitochondrial Antiviral Signaling Protein that Activates NF- $\kappa$ B and IRF3. *Cell*;122(5):669-682.10.1016/j.cell.2005.08.012.<http://dx.doi.org/10.1016/j.cell.2005.08.012>
28. Patsch C, Challet-Meylan L, Thoma EC, Urich E, Heckel T, O'Sullivan JF, Grainger SJ, Kapp FG, Sun L, Christensen K and others. Generation of vascular endothelial and smooth muscle cells from human pluripotent stem cells. *Nat Cell Biol* 2015;17(8):994-1003.10.1038/ncb3205.<https://www.ncbi.nlm.nih.gov/pubmed/26214132>
29. Loh KM, Chen A, Koh PW, Deng TZ, Sinha R, Tsai JM, Barkal AA, Shen KY, Jain R, Morganti RM and others. Mapping the Pairwise Choices Leading from Pluripotency to Human Bone, Heart, and Other Mesoderm Cell Types. *Cell*;166(2):451-467.10.1016/j.cell.2016.06.011.<http://dx.doi.org/10.1016/j.cell.2016.06.011>
30. Chen X, Xu F, Zhu C, Ji J, Zhou X, Feng X, Guang S. Dual sgRNA-directed gene knockout using CRISPR/Cas9 technology in *Caenorhabditis elegans*. *Scientific Reports* 2014;4:7581.10.1038/srep07581  
<http://www.nature.com/articles/srep07581#supplementary-information>.<http://dx.doi.org/10.1038/srep07581>
31. Olsson R, Carlsson P-O. The pancreatic islet endothelial cell: Emerging roles in islet function and disease. *The International Journal of Biochemistry & Cell Biology* 2006;38(5-6):710-714.<http://dx.doi.org/10.1016/j.biocel.2006.02.004>.<http://www.sciencedirect.com/science/article/pii/S1357272506000537>
32. John Wiley & Sons I. CD Antigens. *Current Protocols*; 2000-2010.

- 
33. Nejentsev S, Walker N, Riches D, Egholm M, Todd JA. Rare Variants of IFIH1, a Gene Implicated in Antiviral Responses, Protect against Type 1 Diabetes. *Science (New York, N.Y.)* 2009;324(5925):387-389.10.1126/science.1167728.<http://www.ncbi.nlm.nih.gov/pmc/articles/PMC2707798/>
34. Downes K, Pekalski M, Angus KL, Hardy M, Nutland S, Smyth DJ, Walker NM, Wallace C, Todd JA. Reduced expression of IFIH1 is protective for type 1 diabetes. *PLoS One* 2010;5(9).10.1371/journal.pone.0012646.<https://www.ncbi.nlm.nih.gov/pubmed/20844740>
35. Wu B, Peisley A, Richards C, Yao H, Zeng X, Lin C, Chu F, Walz T, Hur S. Structural Basis for dsRNA Recognition, Filament Formation, and Antiviral Signal Activation by MDA5. *Cell* 2013;152(1–2):276-289.<http://dx.doi.org/10.1016/j.cell.2012.11.048>.<http://www.sciencedirect.com/science/article/pii/S0092867412014365>
36. Shigemoto T, Kageyama M, Hirai R, Zheng J, Yoneyama M, Fujita T. Identification of Loss of Function Mutations in Human Genes Encoding RIG-I and MDA5: IMPLICATIONS FOR RESISTANCE TO TYPE I DIABETES. *Journal of Biological Chemistry* 2009;284(20):13348-13354.10.1074/jbc.M809449200.<http://www.jbc.org/content/284/20/13348.abstract>
37. Berke IC, Yu X, Modis Y, Egelman EH. MDA5 assembles into a polar helical filament on dsRNA. *Proceedings of the National Academy of Sciences* 2012;109(45):18437-18441.10.1073/pnas.1212186109.<http://www.pnas.org/content/109/45/18437.abstract>
38. Berke IC, Li Y, Modis Y. Structural basis of innate immune recognition of viral RNA. *Cellular Microbiology* 2013;15(3):386-394.10.1111/cmi.12061.<http://dx.doi.org/10.1111/cmi.12061>
39. Kumar A, Zhang J, Yu FS. Toll-like receptor 3 agonist poly(I:C)-induced antiviral response in human corneal epithelial cells. *Immunology* 2006;117(1):11-21.10.1111/j.1365-2567.2005.02258.x.<https://www.ncbi.nlm.nih.gov/pubmed/16423036>
40. Sanjana NE, Shalem O, Zhang F. Improved vectors and genome-wide libraries for CRISPR screening. *Nat Meth* 2014;11(8):783-784.10.1038/nmeth.3047  
<http://www.nature.com/nmeth/journal/v11/n8/abs/nmeth.3047.html#supplementary-information>.<http://dx.doi.org/10.1038/nmeth.3047>
41. 2017 Addgene - Homepage. <<http://www.addgene.org/>>.
-

## Annex

**Supplemental Figure 1: Plasmids used in this study.**

A) lentiGuide-Puro plasmid<sup>40</sup> (Addgene plasmid #52963): was used for cloning CRISPR gRNAs; B) pCas9\_GFP (Addgene plasmid #44719): was used in combination with the CRISPR gRNA containing plasmids to specifically cleave target DNA. Both depictions can be found on [www.addgene.org](http://www.addgene.org)<sup>41</sup>.

**Supplemental Table 1: List of gRNAs used.**

This table contains all oligonucleotide sequences that were used to clone the respective CRISPR gRNAs into lentiGuide puro plasmids. The predominately used ones are in bold. The gRNA sequence is in uppercase and the vector backbone is in lower case.

Name	Gene	Direction	Sequence
<b>CR1</b>	<i>IFIH1</i>	forward	caccgGCTAAGTGGGCAGCGGACAG
<b>CR1</b>	<i>IFIH1</i>	reverse	aaacCTGTCCGCTGCCCACTTAGc
CR2	<i>IFIH1</i>	forward	caccGTCCCGCAGACAACAGCACC
CR2	<i>IFIH1</i>	reverse	aaacGGTGCTGTTGTCTGCGGGAC
CR3	<i>IFIH1</i>	forward	caccgGAGACGAGAATTTCCGCTAT
CR3	<i>IFIH1</i>	reverse	aaacATAGCGGAAATTCTCGTCTCc
<b>CR4</b>	<i>IFIH1</i>	forward	caccgGAGGGTGAAAATGTACATCC
<b>CR4</b>	<i>IFIH1</i>	reverse	aaacGGATGTACATTTTCACCCTCc
CR11	<i>IFIH1</i>	forward	caccgGCAGTGTGCTAGCCTGTTC
CR11	<i>IFIH1</i>	reverse	aaacGAACAGGCTAGCACACTGCc
<b>CR12</b>	<i>IFIH1</i>	forward	caccGCAACCTGCTTCACCCCTTG

<b>CR12</b>	<i>IFIH1</i>	reverse	aaacCAAGGGGTGAAGCAGGTTGc
CR13	<i>IFIH1</i>	forward	caccgGGGTTATTCTTGTAATGCT
CR13	<i>IFIH1</i>	reverse	aaacAGCATTACAAGAATAACCCc
<b>CR14</b>	<i>IFIH1</i>	forward	caccgTCTGGACTCACTTGAATTC
<b>CR14</b>	<i>IFIH1</i>	reverse	aaacAATTCAAGTGAGTCCAGAc

**Supplemental Table 2: List of primers.**

This table compiles all primer sequences to amplify *IFIH1*, in both PCR and qPCR, and some downstream signaling proteins in qPCR.

<b>Gene</b>	<b>Application</b>	<b>Direction</b>	<b>Sequence</b>
<i>IFIH1</i>	PCR	forward	CCTGTGGACAACCTCGTCAT
<i>IFIH1</i>	PCR	reverse	CCCTTCTCCAAGGTGCTCAG
<i>IFIH1</i>	PCR	reverse	ACCTCTCAAGGGGCATGTTG
<i>IFIH1</i>	qPCR	forward	TCACAAGTTGATGGTCCTCAAGT
<i>IFIH1</i>	qPCR	reverse	CTGATGAGTTATTCTCCATGCCC
<i>IFNB</i>	qPCR	forward	GTCACTGTGCCTGGACCATAG
<i>IFNB</i>	qPCR	reverse	GTTTCGGAGGTAACCTGTAAGTC
<i>IL-6</i>	qPCR	forward	CCTGAACCTTCCAAAGATGGC
<i>IL-6</i>	qPCR	reverse	TTCACCAGGCAAGTCTCCTCA
<i>IL-8</i>	qPCR	forward	ACTGAGAGTGATTGAGAGTGGAC
<i>IL-8</i>	qPCR	reverse	AACCCTCTGCACCCAGTTTTTC
<i>TNF</i>	qPCR	forward	GAGGCCAAGCCCTGGTATG
<i>TNF</i>	qPCR	reverse	CGGGCCGATTGATCTCAGC
<i>IP10</i>	qPCR	forward	GTGGCATTCAAGGAGTACCTC
<i>IP10</i>	qPCR	reverse	TGATGGCCTTCGATTCTGGATT
<i>OAS</i>	qPCR	forward	TGTCCAAGGTGGTAAAGGGTG
<i>OAS</i>	qPCR	reverse	CCGGCGATTTAACTGATCCTG

**Supplemental Table 3: List of antibodies used for Flow Cytometry.**

*This table contains all antibodies used for quality control of the HuES8 derived ECs.*

<b>Antibody</b>	<b>Clone</b>	<b>Species</b>	<b>Company</b>	<b>Isotype</b>	<b>Channel</b>	<b>Dilution</b>
Anti-CD31	WM59	Mouse	BD Pharmingen	IgG1	FITC	1:200
Anti-CD31	WM59	Mouse	BioLegend	IgG1	APC	1:200

**Supplemental Table 4: List of antibodies used for Western blot.**

*This table compiles all primary and secondary antibodies used to detect MDA5 and  $\alpha$ -actin, as a loading control, expression in wildtype and knockout cells.*

<b>Antibody</b>	<b>Species</b>	<b>Company</b>	<b>Catalog No.</b>	<b>Dilution</b>
Anti-MDA5	Rabbit	Cell Signaling	5321	1:1000
Anti- $\alpha$ -Actin	Mouse	Santa Cruz	Sc-130616	1:1000
Anti-rabbit IgG	Goat	R&D Systems	HAF008	1:3000
Anti-mouse IgG	Donkey	R&D Systems	HAF018	1:3000